

THE UNIVERSITY OF MICHIGAN  
INDUSTRY PROGRAM OF THE COLLEGE OF ENGINEERING

CAPILLARY PENETRATION OF LIQUIDS BETWEEN DISSIMILAR SOLIDS

William J. O'Brien

A dissertation submitted in partial fulfillment  
of the requirements for the degree of  
Doctor of Philosophy in the  
University of Michigan  
Department of Chemical and Metallurgical Engineering  
1967

April, 1967

IP-773

## ACKNOWLEDGMENTS

The author wishes to express his appreciation:

To Professor Robert G. Craig for his advice and guidance during the entire course of this investigation.

To Professor William I. Higuchi for his suggestions involving the mathematical model and radioactivity experiments.

To Professor Floyd A. Peyton for his encouragement and suggestions concerning the application of the findings to dentistry.

To Professor Edwin H. Young for his advice concerning the experimental design and presentation of results.

To Assistant Professor George Zografi for his lectures in surface chemistry.

In addition, acknowledgment is due to the United States Public Health Service for support through PHS Grant DE 177-01 which was administered by Marquette University.

Thanks are also due to the Micrometrical Division of the Bendix Corporation for assistance in obtaining the surface profiles.

## TABLE OF CONTENTS

	<u>Page</u>
ACKNOWLEDGEMENTS.....	ii
LIST OF TABLES.....	v
LIST OF FIGURES.....	vi
NOMENCLATURE.....	viii
 Chapter	
I. INTRODUCTION.....	1
II. LITERATURE REVIEW.....	3
A. Wetting of Solid by Liquid.....	3
B. Capillary Penetration.....	5
C. Fluid Leakage Around Dental Restorations.....	10
1. Radioisotope Penetration.....	11
2. Air Pressure.....	14
3. Dye Penetration.....	15
4. Bacterial Penetration.....	16
5. Percolation.....	17
D. Denture Retention.....	18
III. THEORETICAL STUDY.....	20
A. Mathematical Model.....	20
B. Dimensional Analysis.....	24
C. Role of Mathematical Model.....	24
IV. EXPERIMENTAL.....	27
A. Experimental Design.....	27
B. Measurement of Parameters.....	28
1. Contact Angles.....	28
2. Surface Tension.....	32
3. Capillary Rise.....	32
4. Surface Profile.....	32
C. Radioisotope Penetration.....	34

TABLE OF CONTENTS (CONT'D)

	<u>Page</u>
V. EXPERIMENTAL RESULTS.....	39
A. Parameters.....	39
1. Contact Angles.....	39
2. Surface Tension.....	39
3. Capillary Rise.....	39
4. Surface Profile.....	41
B. Radioisotope Penetration.....	41
VI. EVALUATION OF THE MODEL.....	68
A. Regression Analysis.....	68
B. Correlation Coefficient.....	71
VII. DISCUSSION AND APPLICATION OF RESULTS.....	74
A. General Discussion of Proposed Equation.....	74
B. Leakage of Wax Fillings.....	75
C. Leakage Around Dental Materials.....	78
D. Denture Retention.....	80
VIII. SUMMARY.....	81
REFERENCES.....	84

## LIST OF TABLES

<u>Table</u>		<u>Page</u>
1	Factorial Design Table For Capillary Rise Experiments.....	29
2	Contact Angles of Liquids on Various Solids at 27°C.....	40
3	Radioactivity Counts Per Ten Minutes For Treatments of Extracted Teeth.....	42
4	Analysis of Variances For Radioactivity Counts For Different Treatments.....	43
5	Results of Duncan's New Multiple Range Test For Radioactivity Differences.....	44
6	Predicted and Observed $x_h$ Values, sq. cm.....	69
7	Analysis of Variance For Regression.....	72
8	Values of $\Delta F^S$ For The Penetration of Water Between Dentin ( $\theta = 50^\circ$ ) and Various Materials.....	79

LIST OF FIGURES

<u>Figure</u>		<u>Page</u>
1	Advancing and Receding Contact Angles on a Tilted Plate..	6
2	Capillary Rise Between Plates at an Angle.....	9
3	Capillary Rise Between Dissimilar Parallel Plates.....	21
4	Plan for Development and Evaluation of Mathematical Model.....	26
5	Micromanipulator Used for Contact Angle Measurements.....	31
6	Surface Finish Analyzer.....	33
7	Treatments Applied to Extracted Teeth.....	35
8	Tooth Immersed in Radioactive Solution for Penetration Tests.....	36
9	Liquid Scintillation Spectrometer.....	38
10	Capillary Rise Curves for: (a) Glass-Water-Glass, (b) Silicone-Water-Glass, (c) Teflon-Water-Glass.....	46
11	Capillary Rise Curves for: (a) Glass-Water-Glass, (b) Glass-Water-Acrylic.....	47
12	Capillary Rise Curve for Glass-Water-Silicone.....	48
13	Capillary Rise Curve for Acrylic-Water-Acrylic.....	49
14	Capillary Rise Curve for Vista-Water-Vista.....	50
15	Capillary Rise Curve for Glass-Water-Glass.....	51
16	Capillary Rise Curve for Silicone-Water-Acrylic.....	16
17	Capillary Rise Curve for Vista-Water-Vista.....	53
18	Capillary Rise Curve for Glass-Water-Acrylic.....	54
19	Capillary Rise Curve for Glass-Water-Glass.....	55
20	Capillary Rise Curve for Glass-Ethanol-Glass.....	20

LIST OF FIGURES (CONT'D)

<u>Figure</u>		<u>Page</u>
21	Capillary Rise Curve for Acrylic-Ethanol-Glass.....	21
22	Capillary Rise Curve for Acrylic-Ethanol-Teflon.....	22
23	Capillary Rise Curve for Glass-Ethanol-Acrylic.....	59
24	Capillary Rise Curve for Acrylic-Ethanol-Glass.....	60
25	Capillary Rise Curve for Acrylic-Ethanol-Acrylic.....	61
26	Capillary Rise Curve for Acrylic-Iodobenzene-Acrylic.....	62
27	Capillary Rise Curve for Teflon-Iodobenzene-Acrylic.....	63
28	Capillary Rise Curve for Acrylic-Iodobenzene-Glass.....	64
29	Capillary Rise Curves for: (a) Glass-Iodobenzene-Glass, (b) Teflon-Iodobenzene-Glass.....	65
30	Capillary Rise Curve for Acrylic-Iodobenzene-Glass.....	66
31	Surface Profiles Obtained From Surface Analyzer.....	67
32	Regression of Observed $xh$ Values on Calculated $xh$ Values.....	70
33	Observed $xh$ Values Versus Interface Free Energy Change Per Unit Area for Water.....	76
34	Capillary Rise Curves for Water Between Two Plates for Different $(\cos\theta_1 + \cos\theta_2)$ Values.....	77

## NOMENCLATURE

A	Area in sq. cm.
b	Distance between plates, centimeters.
d	Liquid density, g/cm <sup>3</sup> .
f	Force in dynes.
F	Ratio of variances.
$\Delta F^S$	Interfacial free energy change per unit area, ergs/cm <sup>2</sup> .
$F_{SL}$	Interfacial free energy at a solid-liquid interface, ergs/cm <sup>2</sup> .
$F_{SA}$	Interfacial free energy at a solid-air interface, ergs/cm <sup>2</sup> .
g	Gravitational constant, 980 cm/sec <sup>2</sup> .
h	Capillary rise, centimeters.
hx	Product of distance, x, from vertex and height of meniscus above liquid level.
r	Radius of curvature, centimeters.
t	Student's t is a statistical measure of differences between means.
x	Distance from vertex of plates, cm.
$\Delta P$	Pressure difference, dynes/cm <sup>2</sup> .
$\gamma_{LV}$	Interfacial tension or surface tension at a liquid-vapor interface, dynes/cm, equivalent energy dimensions, ergs/cm <sup>2</sup> .
$\gamma_{SA}$	Interfacial energy at a solid-air interface, ergs/cm <sup>2</sup> .
$\gamma_{SL}$	Interfacial energy at a solid-liquid interface, ergs/cm <sup>2</sup> .
$\phi$	Angle between plates, minutes.
$\theta$	Contact angle, degrees.
$F_{SV}$	Interfacial free energy at a solid-vapor interface, ergs/cm <sup>2</sup> .



## I. INTRODUCTION

Capillary penetration of liquids into narrow tubes and crevices has been a subject of interest since DaVinci. This phenomenon has many biologic implications. In the field of dentistry, the penetration of a thin film of saliva between the palate and the surface of a complete denture has been identified as one of the principal sources of denture retention. A similar situation exists when contact lenses are placed in the eyes; lachrymal fluids are chiefly responsible for retention. In both of these cases this penetration is necessary for the success of the prosthetic device.

In contrast, the penetration of mouth fluids between a filling and dentin or enamel is considered undesirable. This penetration is made possible by the lack of adhesion between the present filling materials and tooth structure. Leakage around fillings is believed to cause secondary recurrent caries and subsequent pulpal degeneration since bacterial products are carried along with the liquid.

Since these capillary phenomena occur within the body, they are difficult to study. As a result, capillary penetration around prosthetic materials is poorly understood. One approach is to set up simplified mathematical models to describe these processes. This is the focus of the present research. Pursuant to this aim, an attempt is made in this research to derive an equation for capillary penetration between dissimilar materials. Predictions based on this equation are compared with experimental results for specific capillary systems by means of statistical decision techniques.

In summary, the specific aims of this research were as follows:

1. To derive a mathematical model describing the capillary penetration of a liquid into a crevice composed of two dissimilar plates.
2. To evaluate the ability of the proposed equation to predict capillary rise. This stage involves the comparison between predicted and observed values by means of statistical analysis.
3. To apply the proposed model to the problems of penetration around dental fillings and complete dentures. This involves experimenting with the mathematical model and considering hypothetical situations for heuristic purposes.

## II. LITERATURE REVIEW

### A. Wetting of Solid by Liquid

According to Bartell<sup>(1)</sup>, wetting occurs when a solid phase and a liquid phase come into contact in any manner so as to form a solid-liquid interface. If a drop of water is placed on a flat surface of a low energy solid, such as polyethylene, a contact angle will be formed. The magnitude of this contact angle,  $\theta$ , is a measure of the degree of wetting of the solid by the liquid. After equilibrium has been established, the Young equation<sup>(2)</sup> may be used to define the contact angle in terms of the surface tensions involved:

$$\gamma_{SA} = \gamma_{SL} + \gamma_{LV} \cos\theta, \quad (1)$$

where  $\gamma_{SA}$  represents the interfacial tension between the solid and air,  $\gamma_{SL}$  is the interfacial tension between solid and liquid and  $\gamma_{LV}$  is the surface tension of the liquid.

Difficulties are encountered with the concept of a tension acting along a solid surface. More correctly surface energy per unit area terms should be substituted for the surface tension terms in the Young equation.<sup>(2)</sup>

$$F_{SA} = F_{SL} + \gamma_{LV} \cos\theta \quad (2)$$

Soft solids, solids of low free surface, are generally poorly wetted by liquids. Paraffin wax a low energy solid, is poorly wetted by water producing a contact angle of about  $110^\circ$ .<sup>(3)</sup> Contact angles of water on metals, high energy solids, are usually below  $10^\circ$ . Water on poly-(methyl methacrylate) has a contact angle value of around  $75^\circ$  whereas the value of poly-(tetrafluoroethylene) is around  $118^\circ$ .

The roughness of the solid surface has been found to have an influence on the observed contact angle. Shepard<sup>(4)</sup> found the contact angle of water on paraffin was increased from  $97^\circ$  to  $110^\circ$  by roughening the surface. In general, roughening the surface of the solid has the effect of making the observed angle differ more from  $90^\circ$ . When the contact angle on a smooth solid is less than  $90^\circ$ , roughening the solid surface will reduce the observed angle. The effect on a surface with a contact angle greater than  $90^\circ$  would be an increase of the observed angle.

Adsorption also has an important effect on the magnitude of the contact angle.<sup>(5)</sup> If the solid adsorbs vapor, the surface energy will be reduced. Adsorption of impurities in the liquid phase at the solid-liquid interface tends to lower the interfacial energy. The new values of  $F_{SV}$ ,  $F_{SL}$  and  $\gamma_{LV}$  produced by adsorption will determine the new contact angle.

The contact angle of a liquid advancing across a solid surface is usually greater than the angle observed when the liquid advances over a surface wetted by the same liquid. This difference has been termed hysteresis and may be quite high in some systems. Several theories have been presented to explain this phenomenon. Davies<sup>(6)</sup> argues that the larger advancing contact angle may be due to a film of some material which prevents the liquid from adhering to the solid. Upon contact with the liquid this film is removed, giving a smaller receding angle. It has been found that a film of greasy material is usually adsorbed by solids standing in air. Less than monolayer coverage will produce significant changes in surface energy. Advancing and receding contact angles

may be determined by the method of Macdougall and Ockrent.<sup>(7)</sup> A drop of the liquid is placed on the solid and the solid is then tilted at an angle to the horizontal. The advancing and receding angles are measured at the angle of tilt just sufficient to prevent the drop from sliding down the plane, as shown in Figure 1.

### B. Capillary Penetration

If a glass tube of small diameter is placed in a vessel of water, the water will rise in the tube to a height given by the following equation within limits:<sup>(8)</sup>

$$h = \frac{2\gamma_{LV}\cos\theta}{g r d} , \quad (3)$$

where  $d$  is the density of the liquid,  $h$  is the height of rise,  $\gamma_{LV}$  is the liquid surface tension,  $\theta$  represents the contact angle,  $g$  is the gravitational constant, and  $r$  is the radius of the tube. If the contact angle of the liquid on the wall of the tube exceeds  $90^\circ$ , the liquid will be depressed in the tube. At least two methods of attack have been used to derive this equation. Young and Laplace<sup>(9)</sup> equated the increase in free energy resulting from an expansion of a concave liquid surface to the pressure - volume work accompanying the expansion. This approach is based upon an analogy with the curvature of the liquid interface formed by blowing a bubble beneath a liquid surface. The resulting equation is:

$$\Delta P = \gamma_{LV} (1/r_1 + 1/r_2) , \quad (4)$$

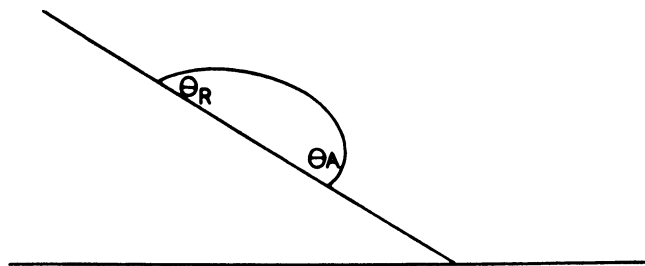


Figure 1. Advancing and Receding Contact Angles on a Tilted Plate.

Here,  $r_1$  and  $r_2$  are the principal radii of curvature of the bubble and  $\Delta P$  is interpreted as the decrease in pressure below a concave meniscus. If the concave meniscus is perfectly spherical, the two radii of curvature will be equal, and the equation reduces to:

$$\Delta P = 2 \gamma_{LV}/r \quad (5)$$

This "decrease in pressure" below the meniscus in a capillary tube was equated to the increase in hydrostatic pressure accompanying the rise of liquid in the tube at equilibrium,

$$\Delta P = 2 \gamma_{LV}/r = dgh , \quad (6)$$

and by rearranging terms,

$$h = 2 \gamma_{LV}/dgr . \quad (7)$$

If the liquid does not wet the surface of the tube completely, i. e., the contact angle is greater than zero, the radii of the meniscus will be given by  $r/\cos\theta$  .

Another correction factor is introduced for the weight of the liquid meniscus.<sup>(10)</sup> If the contact angle is zero this will be  $r/3$  . The equation may then be rewritten as:

$$(h + r/3) = \frac{2 \gamma_{LV} \cos\theta}{d g r} \quad (8)$$

This latter correction factor is usually not necessary with tube diameters less than one millimeter. For larger tubes, correction factors have been derived by Bashforth and Adams.<sup>(11)</sup>

The Young and Laplace equation may be applied to the case of penetration between two parallel vertical plates, however, the diameter of the crevice space,  $b$ , is substituted for the radius.

Another concept concerning the surfaces of liquids was introduced in the 17th Century by Franciscus Linus.<sup>(12)</sup> Linus put forth the hypothesis of an invisible membrane on the surface of liquids. If the surface tension of this membrane is considered as pulling the liquid up the capillary space,  $b$ , between two parallel plates, then

$$2 \gamma_{LV} = b d g h . \quad (9)$$

Rearranging, the capillary equation is obtained,

$$h = \frac{2 \gamma_{LV}}{b d g} . \quad (10)$$

The mathematical similarity with the Young-Laplace equation for capillary rise and the rise between parallel plates is complete.

The penetration of liquids between two vertical plates inclined at a slight angle produces interesting effects. Humphry Ditton (Reference 13) showed in 1729 that the liquid surface between two plates placed in the aforementioned arrangement described a hyperbola. This technique was refined by Grunmach<sup>(14)</sup> and used as a means for determining surface tension. If  $\phi$  is the angle between the plates as illustrated in Figure 2, the distance between the plates,  $b$ , at a distance,  $x$ , from the vertex is

$$b = 2 x \tan \phi/2 . \quad (11)$$



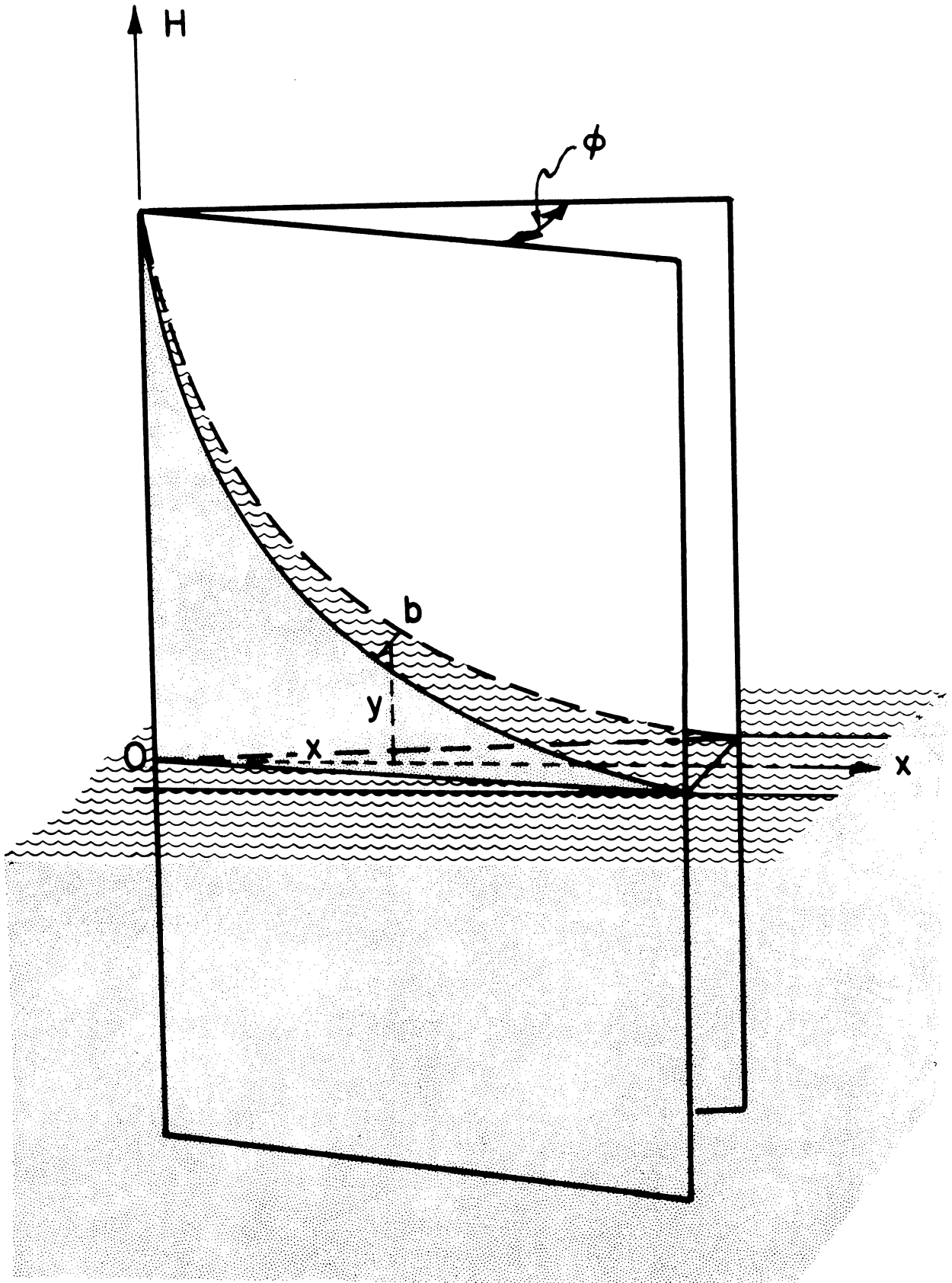


Figure 2. Capillary Rise Between Plates at an Angle.

Substituting this expression into the capillary equation,

$$h = \frac{\gamma_{LV} \cos\theta}{g d x \tan \phi/2} . \quad (12)$$

This relation may be rearranged to give the equation of a rectangular hyperbola:

$$xh = \frac{\gamma_{LV} \cos\theta}{g d \tan \phi/2} . \quad (13)$$

By determining  $xh$  at several points along the surface of the liquid and averaging them, the surface tension of a liquid may be calculated. This technique has been applied to measure the surface tensions of a variety of liquids including water, benzene, toluene, and mercury with fairly good agreement with the results of other methods. (References 14 and 15)

In all of the previous discussion, an assumption was made that the plates used were of the same material. If in lieu of the single species of material, there are two dissimilar plates, the aforementioned equations fail to apply. Bakker<sup>(16)</sup> has considered this situation and attempted, without success, to apply the Young-Laplace curvature approach. Due to the complex curvature of the liquid-vapor surface, the radius of curvature is constantly changing from one point to another. Wolf,<sup>(17)</sup> considering the same problem, stated that the capillary penetration between dissimilar plates is poorly understood.

### C. Fluid Leakage Around Dental Restorations

It is generally considered that the present restorative materials used in dentistry do not adhere to tooth structure. As a result

of this lack of joint strength, a separation could exist between the restoration and the tooth into which mouth fluids may penetrate. Recurrent caries beneath restorations has been attributed to this fluid exchange. It is therefore of interest to measure the amount of marginal penetration found with various restorative materials. Several tests have been devised which propose to accomplish this purpose. They may be classified into several categories as follows:

1. radioisotope penetration,
2. air pressure,
3. dye penetration,
4. bacterial penetration,
5. percolation.

A description of each method will be given along with some typical results obtained by use of the technique.

1. Radioisotope Penetration: Phillips<sup>(18)</sup>, and associates, employed  $^{45}\text{Ca}$  to assess the marginal leakage of several restorative materials. The restorations were placed in sound, extracted teeth. They were then stored in tap water to prevent dehydration. In order to minimize penetration of the isotope along the root canal, cuspids and bicuspid were utilized. The materials studied were: amalgam, silicate cement, zinc phosphate cement, and acrylic resins. All of the restorations were carved but were not polished. A radioactive solution of 0.1 millicuries per milliliter of calcium chloride was used. The pH was adjusted to 5.5 by adding dilute NaOH. The roots, root canals and discrepancies in the enamel surfaces were "sealed" with tin foil and nail lacquer. Only the margins of the restoration were exposed to the solution.

The teeth with roots filled, were immersed in the calcium chloride solution for two hours, rinsed in water and cleaned with a detergent. Longitudinal sections were prepared by using a wet 400 mesh carborundum wheel. The pulp was removed from the specimens and cut surfaces were brushed and dried. The surfaces were then placed in contact with x-ray film. An autoradiograph was formed where the film was exposed to the radiation to the isotope. The film and specimen were left in contact with each other for 17 hours before development. Isotope infiltration was indicated by dark areas on the autoradiograph. The margins of the 24-hour amalgam restorations were readily penetrated by the isotope. Leakage appeared to diminish with aging of the restoration. Also, cavity varnishes appeared to diminish the amount of penetration. Some leakage was observed with all silicate and zinc phosphate cement restorations. The use of a cavity liner improved the adaption of resin restorations. Penetration was more evident when the restorations were subjected to thermal change.

Lyell, Barber, and Massler<sup>(19)</sup> used isotopes of sulfur and calcium for penetration studies. Class V amalgam cavities were filled with silver amalgam in ninety-three freshly extracted teeth that had been stored in tap water. The teeth were stored in the following solutions: sodium sulfide, saliva, tap water, and distilled water.

After storage, the roots of the teeth were covered with wax and the crowns then were immersed in dye/isotope solution for 1 week. The dye was a 3.8% solution of toluidine blue, and the strength of the isotope solution was 50 microcuries per cubic centimeter for  $^{35}\text{S}$  and 20 microcuries per c.c. for  $^{45}\text{Ca}$ . Preparation of the teeth for autoradiography and for microscopic examination was as described by Going.<sup>(20)</sup>

The teeth were cut in hemisections through the center of each filling on a special machine. Each hemisection was then placed on fast dental x-ray film to obtain autoradiographs. At least one overexposed and one underexposed autoradiograph were obtained in order to judge proper exposure and maximal depth of marginal penetration by each isotope. Each specimen was then examined under a binocular dissecting microscope at 10-40 magnifications to determine the depth of dye penetration. As in the previous studies, specimens filled with amalgam and placed immediately into the dye/isotope solution showed penetration of the isotope through the margins and into the underlying dentin in 80 per cent of the specimens examined.

Cantwell and associates<sup>(21)</sup> sought to determine if molecular size was an important factor in penetration. A four-walled cavity preparation was placed in the labial surface of extracted anterior teeth. After placement of the amalgam restoration, the teeth were placed in a humidior for 24 hours. When the restorations were polished, the teeth were placed in solutions of labeled fructose for intervals up to 24 hours. Sectioning of the teeth was done in a bucco-lingual plane and exposed to radiographic film for 48-72 hours. These tests indicated a fine line of exposure around the majority of the restorations.

Going and Massler<sup>(22)</sup> used the radioisotope technique to study the effectiveness of varnish in preventing marginal penetration. Four isotopes were used:  $^{131}\text{I}$ ,  $^{35}\text{S}$ ,  $^{45}\text{Ca}$ ,  $^{22}\text{Na}$ . They tested: copal resin varnish, polystyrene-ethyl cellulose liner, calcium hydroxide liners, zinc-oxide eugenol cement and zinc phosphate cement.

Penetration of all four types of isotopes took place with all of the specimens. They found that  $^{35}\text{S}$  produced the sharpest and most detailed autoradiographs.

2. Air Pressure: The investigators chiefly responsible for this technique were Fiasconaro and Sherman.<sup>(23)</sup> In this test, a class V (gingival cavity) was prepared and filled with one of the materials to be tested. The root of the tooth is cut away from the crown about one millimeter apical to the cervical line. Next the pulp chamber is enlarged so that it makes contact with the filling. Using compound impression material, a brass tube is sealed into the pulpal chamber on one end and attached to a rubber hose at the other end. This setup is immersed in water. Air pressure is then applied to the pulp chamber through the hose attached to the brass tube. The pressure is gradually increased until bubbles form at the cavo-surface margin. This pressure is recorded in pounds/sq. in. According to the thinking of the authors mentioned above, the higher the pressure necessary to produce bubbles, the better is the marginal seal. They found that none of the gold foil or zinc oxy-phosphate cements showed signs of leakage. With dental amalgam, they found that one leaked at 38 psi. and two others showed no leakage at pressures up to 50 psi. Gold inlays that had been cemented with zinc oxy-phosphate failed to show leakage until 45 psi. was reached. On the other hand, two gold inlays that were cemented using a self-curing resin leaked at 20 psi. and at 50 psi. Two silicate cement restorations resisted leakage until 38 psi. was reached. The acrylic resin restorations were the least sealing of the materials tested. They leaked at values of 6 psi.

3. Dye Penetration: This technique for detecting marginal leakage is similar to the method using radioisotopes. An extracted tooth is prepared and filled with the restorative material. It is then immersed in a solution containing the dye. After remaining in the solution for several hours, the tooth is removed and sectioned for microscopic study. Any penetration of the dye is observed as a coloring at the cavo-surface margin and under the restoration. In a paper previously referred to, Lyell and associates<sup>(19)</sup> used a solution of 3.8% toluidine blue as a dye to test for marginal penetration around amalgam restorations. The sectioned teeth were examined under 10-40 magnifications. Penetration was observed in most of the tests.

Using extracted bovine teeth, Pinto and Buonocore<sup>(24)</sup> utilized the dye penetration test to assess the leakage around amalgam restorations lined with various cavity liners. Class V cavities were filled with amalgam after having been lined with: An adhesive, cavity varnish and zinc oxide in water. The filled teeth were put through a series of thermal cycles from 5°C to 60°C. Again, as in the isotope penetration test, the roots were sealed with wax. Immersion in basic fuchsin dye for 24 hours was followed by cutting the teeth into one millimeter sections. A microscope was then used to examine the sections for penetration of the fuchsin dye. These investigators reported evidence of penetration under fillings that had been lined with the adhesive and cavity varnish. These results are in disagreement with those of other investigators who observed less leakage when the same cavity varnish was used.

Another variation of the dye penetration test was employed by Nelsen, Wolcott and Paffenbarger.<sup>(25)</sup> They placed a few small crystals of fluorescein on the pulpal wall of class V cavities and then filled the cavities. The filled teeth were then put through a temperature change cycle and the liquid exuded from the margins was examined with ultraviolet light for signs of fluorescein. In performing this test with acrylic restorations, they observed fluorescein dye penetration.

4. Bacterial Penetration: Two distinct methods exist for utilizing bacteria to test for marginal leakage. One method, used by Harrison,<sup>(26)</sup> consisted of placing small pieces of sterile filter paper on the cavity floor of prepared teeth and recovering them at a latter time. An aseptic technic was used to place occlusal type silver amalgam restorations in 20 primary mandibular molar teeth in ten patients. One cavity preparation in the tooth of each child was lined with a cavity liner. The other cavity preparation was not lined with a varnish and served as a control. Cultures were taken immediately after the cavity preparation was completed to determine the original bacterial status of the prepared tooth surfaces. Cultures were made of the dentin of each tooth prior to placing the fillings. The disks were recovered after one week. One culture was incubated aerobically and another anaerobically. They found that filter paper disks from all ten teeth in the group that received varnish produced growth. Also, growth was produced in the unlined teeth. *Streptococcus viridans* was present along with coliform organism.



Another method using bacteria was developed by Mortensen, Boucher and Ryge.<sup>(27)</sup> Freshly extracted carious-free teeth were prepared for Class I occlusal restorations. The cavities were filled with amalgam, silicate cement, and zinc phosphate restorations. Next, each tooth was sealed in a plastic tube with an epoxy resin. A hole was drilled from the pulp chamber to the bottom of the restoration, and the roots were cut off. Sterilization then followed with ethylene oxide. A broth culture of *Serratia Marcescens* was added to the tube containing the tooth. The tube was placed into a test tube containing a sterile broth. The tube was subjected to a temperature cycle from 5°C to 37°C. Leakage around the margins was indicated when the sterile broth became cloudy and had the red pigment of the bacteria. About half of the amalgam restorations showed leakage. Data on the other materials tested is not yet available.

5. Percolation: This method has previously been referred to under the dye penetration classification. Essentially, this technique involves observing the margins of a restoration for signs of fluid exchange during thermal cycling. Since restorative materials do not have the same thermal coefficient as tooth structure, a space will develop during temperature changes. For acrylic resin, this channel is estimated to be 10 microns wide. Since the resolution of the eye is in the order of 75 microns, magnification is necessary for the observation of this space. Fluorescein crystals may also be placed under the restoration being studied and the penetration of this dye observed during thermal cycling. In the investigation referred to above, the researchers concluded that temperature changes of teeth and restorations in the mouth

cause a fluid exchange between the teeth and restorations made of gutta-percha, zinc oxide and eugenol cement, silicate cement, zinc phosphate, cement, amalgam, cast gold, gold foil, and acrylic resin. Also, they theorized that marginal penetration of fluids may be an explanation for the recurrence of caries at the margins of restorations.

#### D. Denture Retention

The capillary penetration of a thin film of saliva between the palate and surface of a complete denture has been identified as one of the principal sources of denture retention. Ostlund<sup>(28)</sup> found that the surface tension of the film between the denture and a model affected the retention markedly. He found that thin films gave greater retention. Craig, Berry and Peyton<sup>(29)</sup> measured the adhesion of circular disks of various plastics joined with water and saliva films. They found that the force necessary to separate the disks could be calculated using the formula:

$$f = \frac{2 \gamma_{LV} \cos\theta A}{bg} \quad (14)$$

Where  $A$  is the area of the disk,  $\theta$  is the contact angle of the liquid on the solid and  $b$  is the distance between the plates. O'Brien and Ryge<sup>(30)</sup> studied the effects of coating denture resins with thin films of silica. They found that this treatment made the resin more wettable and thus would tend to improve the retentive forces. Their results showed increase in the force necessary to separate treated resin disks from glass when water joined the two. This increase was attributed to the improved wettability. Equation<sup>(14)</sup> applies to systems in which the liquid wets both solids to the same degree. In this

case, the equation reduces to

$$f = \Delta P A \quad (15)$$

Where  $\Delta P$  represents the capillary pressure. Problems arise when Equation (14) is applied to the force between two dissimilar materials since there may be two different angles of contact. Also, if the viscosity of the film is high, the force becomes time dependent.

### III. THEORETICAL STUDY

#### A. Mathematical Model

The mathematical formulas derived by Young and Laplace cannot be readily applied to the penetration of a liquid between dissimilar solids. Their equation,

$$h = \frac{2 \gamma_{LV}}{d g r} , \quad (3)$$

requires a knowledge of the radius of curvature of the liquid meniscus. Since the radius of curvature of the meniscus in the case of heterogeneous capillary spaces changes from point to point, it is extremely difficult if not impossible to define. Because of the greater efficiency and broader basis for inference that a mathematical model provides, an attempt at developing such a model was made in this study. Consider the heterogeneous capillary space shown in Figure 3. The width of the plates is chosen as one centimeter in order to simplify the calculations of interfacial area. The decrease in surface free energy realized by raising a differential element,  $dh$ , to a level  $h$  may be expressed as the change in surface free energy per unit area multiplied by the area of the solid-liquid interface,  $dA$  :

$$dF = (F_{SV} - F_{SL})_1 dA + (F_{SV} - F_{SL})_2 dA . \quad (16)$$

It is necessary to treat the two solid-liquid interfaces separately since they have different properties. Since the Young-Dupre equation gives

$$(F_{SV} - F_{SL}) = \gamma_{LV} \cos\theta , \quad (17)$$

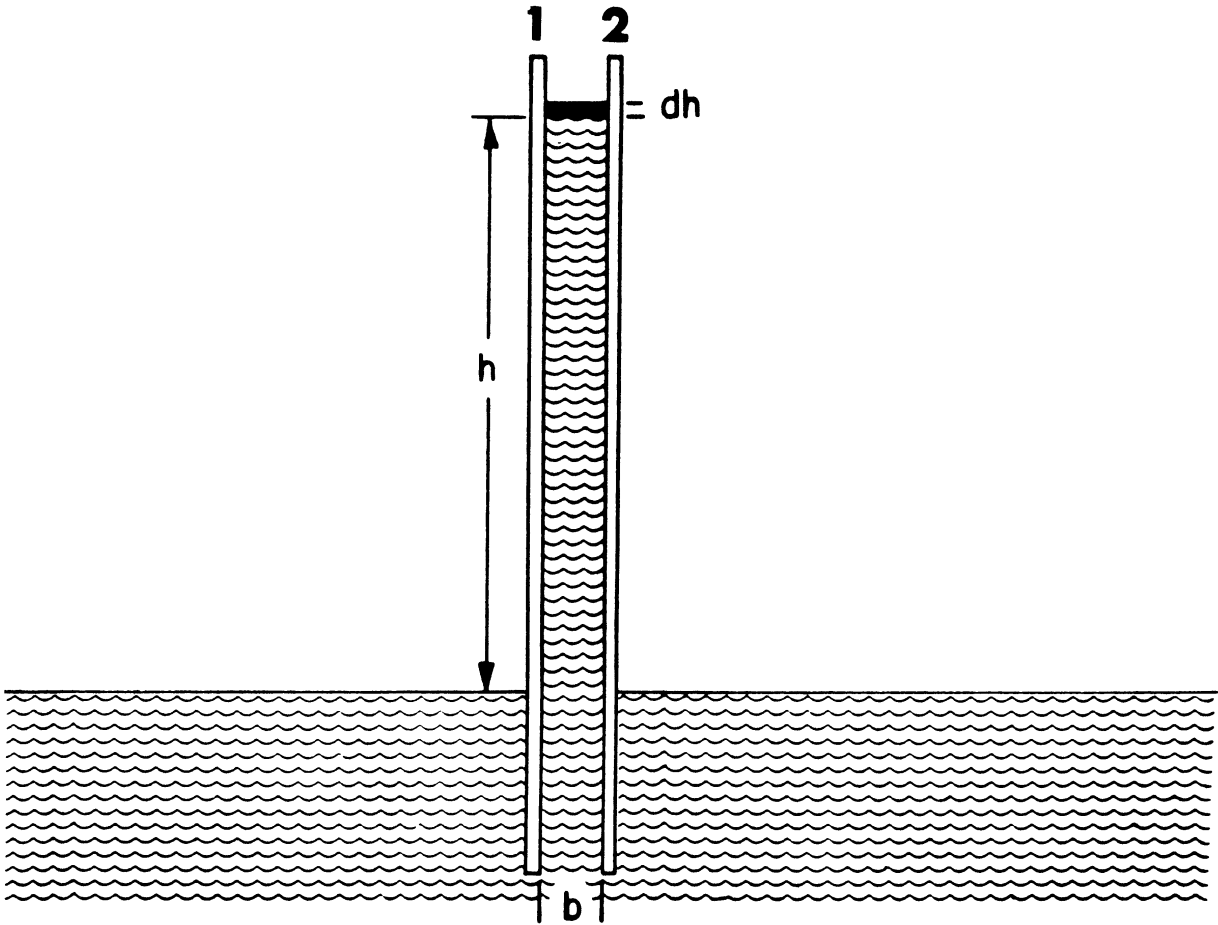


Figure 3. Capillary Rise Between Dissimilar Parallel Plates.

we may write

$$dF = \gamma_{LV} \cos\theta_1 l dh + \gamma_{LV} \cos\theta_2 l dh . \quad (18)$$

By combining terms,

$$dF = \gamma_{LV} (\cos\theta_1 + \cos\theta_2) dh . \quad (19)$$

This may be equated to the increase in gravitational free energy accompanying this rise when equilibrium is reached.

$$\gamma_{LV} (\cos\theta_1 + \cos\theta_2) dh = (dh) (b) (d) (h) (g) . \quad (20)$$

Dividing both sides by  $dh$  , and solving for  $h$  ,

$$h = \frac{\gamma_{LV} (\cos\theta_1 + \cos\theta_2)}{(b) (d) (g)} . \quad (21)$$

This is the capillary equation for a liquid rising between dissimilar plates. If both contact angles are equal, the equation simplifies to

$$h = \frac{2 \gamma \cos\theta}{(b)(d)(g)} . \quad (22)$$

which is in complete agreement with that derived by the Young-Laplace approach. However, it is important to note that no consideration was given to the curvature of the meniscus. Also, the newly obtained prime equation has been derived with the proviso that the amount of liquid in the meniscus is insignificant. This stipulation is also made in the derivation of the Young-Laplace equation, and has been found to hold as long as the capillary space is small. In the case of relatively wide capillary tubes, the size of the meniscus cannot be neglected. Modern interpretation of capillary phenomena favors the surface energy approach

applied in the present derivation of this equation. However, the "surface tension" concept also lends itself toward the development of such a relationship. Consider the weight of liquid held up in a capillary space by the vertical components of surface tension of the liquid for plates 1 centimeter wide:

$$\gamma_{LV} \cos\theta_1 + \gamma_{LV} \cos\theta_2 = hbdg . \quad (23)$$

Solving for  $h$  ,

$$h = \frac{\gamma_{LV} (\cos\theta_1 + \cos\theta_2)}{b d g} . \quad (24)$$

Again, the mathematical identity of the approaches of surface free energy and surface tension is indicated.

Inclined Plates: Since  $b$  , the distance between the plates, varies when they are at an angle in respect to each other, the prime equation must be modified. As previously shown,

$$b = 2 x \tan \phi/2 . \quad (11)$$

Substituting this expression in the prime equation, (21), one obtains

$$h = \frac{\gamma_{LV} (\cos\theta_1 + \cos\theta_2)}{2 d g x \tan \phi/2} . \quad (25)$$

The equation of the hyperbola described by the surface of the liquid is then

$$hx = \frac{\gamma_{LV} (\cos\theta_1 + \cos\theta_2)}{2 d g \tan \phi/2} = K . \quad (26)$$

### B. Dimensional Analysis

Simple dimensional analysis<sup>(32)</sup> may be employed in checking the correctness of these newly derived equations. Equations that have a rational basis and that have been deduced from general considerations are true in all systems of units. This type of an equation is termed a "complete" equation. It has been shown that any complete equation can be put into such form that it is dimensionally homogeneous. To check the homogeneity of the newly derived equation for the capillary penetration between dissimilar plates inclined at an angle with each other, we first reduce it to fundamental units of mass, time and length. Since  $\gamma = MT^{-2}$ ,  $d = ML^{-3}$ ,  $g = LT^{-2}$ ,  $x = L$ ,  $\theta = 0$ , and  $h = L$ , we may write for Equation (26)

$$L = \frac{(MT^{-2})^0}{(ML^{-3})(LT^{-2})(L)(0)} \quad , \quad (27)$$

or

$$L = L .$$

This check gives an indication of the correctness of the derived equation with respect to its dimensions.

### C. Role of the Mathematical Model

An advantage of a model is that it provides a frame of reference for consideration of the problem. The model indicates which real world attributes are important in the system under consideration. A mathematical model serves a heuristic purpose since it leads not to conclusion about physical phenomena but rather to conclusions about what would occur if the system were of the kind assumed. These "would be" conclusions serve as links in the chain of reasoning. If they can be coupled with observations suggested by the reasoning and modified



in accordance with the results of the observations, they can become the building blocks of a future realistic theory. The process of testing a model is indicated in Figure 4. This is the scheme that was followed in this research. The parameters in the present case are indicated by the model as being  $\gamma_{LV}$ ,  $\theta_1$ ,  $\theta_2$ ,  $d$ , and  $b$ . These may be determined in the laboratory for a given system. By utilizing the values of these parameters in the mathematical model, we can arrive at a prediction of the value of  $h_x$  for a given system. In order to test the prediction based upon the model and the measured parameters, an independent measurement of the average  $h_x$  value must be made. This may be obtained by actually measuring the heights to which the liquid will rise between the plates in question. In order to evaluate the model, the degree of association between the predicted values and those measured must be determined. The closeness of the predicted values to the measured values may be determined by statistical significance tests. These statistical tests compare the strength of the effect with an estimate of the error involved in making the tests; a significant degree of association will be found if the closeness of the agreement outweighs the errors involved in the experimental work.

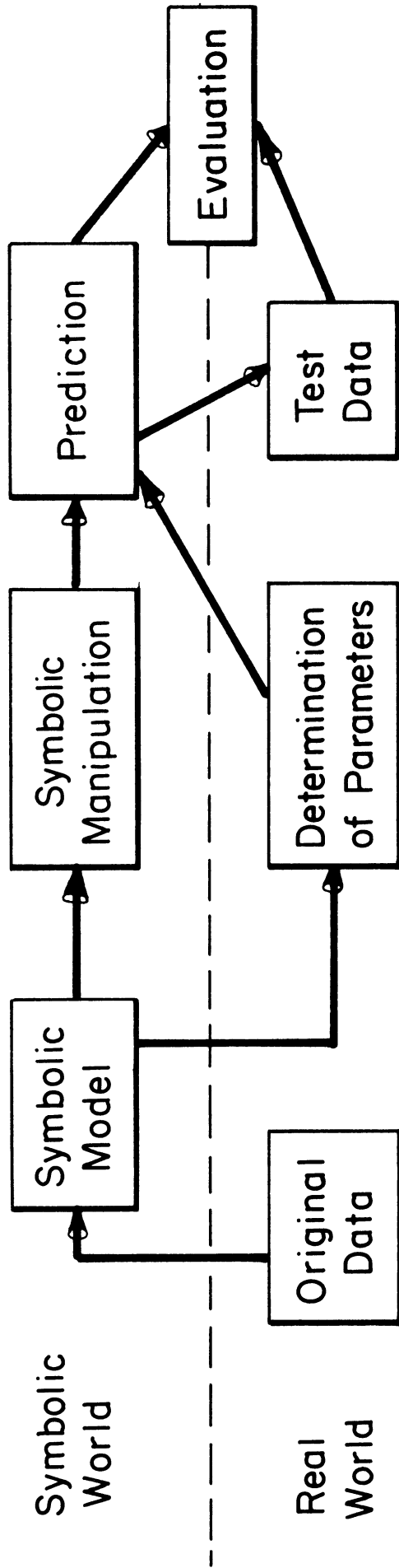


Figure 4. Plan for Development and Evaluation of Mathematical Model.

## IV. EXPERIMENTAL

### A. Experimental Design

The purpose of a research project to a large measure, determines the design of the experiments. Statistical theory has a great deal to say on how experiments should be designed to obtain significant conclusions with a minimum number of experiments. The work of Fisher<sup>(33)</sup> has contributed, to a large degree, toward the present methods of experimental design. In particular, he was responsible for developing the concept of factorial experimentation. This approach stresses the importance of obtaining an accurate estimate of the magnitude of the error variance, rather than its minimization. An accurate estimate of the error variance is necessary in order to apply an exact test of significance. In addition, factorial designs include in the same experiment as many as possible of the factors whose effects are to be determined. Here, is another departure from the classical idea of experimentation. The classical approach is to have all the independent variables but one constant. The advantage of Fisher's approach is greater efficiency in obtaining exact tests of significance. A higher efficiency is obtained since estimates of the effect at a predetermined level of accuracy can be determined in a much smaller total number of observations.

In a factorial design permutations of treatments are examined. Several levels of one factor are crisscrossed with several levels of another. The factors to be introduced in the present research are: wetting of solid 1, wetting of solid 2, and the surface tension of the

liquid. Therefore there are three factors. The factorial design used is shown in Table 1. The yield or effect to be obtained in this experiment is an estimate of capillary rise or pressure. In order to reduce the error variance, the aforementioned hyperbola method was chosen. An average product of distance from the vertex,  $x$ , and the capillary rise at that distance,  $h$ , was chosen as an estimate of the yield. Therefore the error variance was reduced by a factor of  $n^{1/2}$ , when  $n$  was the number of data points per hyperbola. In order to increase the numerical differences between the treatment combinations, materials and liquids with widely different surface energy values were chosen. The span in surface tension between ethanol and water is about 50 dynes/cm. The range of differences in contact angle values on the solids is about  $95^\circ$ .

It was hoped that all of these measures would contribute toward a wider basis of inference, the specific aim being the evaluation of the newly derived mathematical model for the penetration of liquids between dissimilar solids. Pursuant to this goal, another independent estimate of  $xh$  was obtained from Equation (26) by substituting experimental values of  $\theta_1$ ,  $\theta_2$  and  $\gamma_{LV}$  along with known values of  $\phi$  and  $d$ . Comparison between the predicted and observed  $xh$  values were then made with statistical significance tests.

## B. Measurement of Parameters

1. Contact Angles: The inclined plate method was used to measure the advancing and receding contact angles. This method has been developed by Macdougall and Ockrent<sup>(7)</sup>. A drop of the liquid was

TABLE 1  
 FACTORIAL DESIGN TABLE FOR CAPILLARY RISE EXPERIMENTS.

WATER				IODOBENZENE				ETHANOL			
GLASS	TEFLON	ACRYLIC	SILICONE	GLASS	TEFLON	ACRYLIC		GLASS	TEFLON		ACRYLIC
G-W-G	G-W-T	G-W-A	G-W-S	G-I-G	G-I-T	G-I-A		G-E-G	G-E-T		G-E-A
A-W-G	A-W-T	A-W-A	A-W-S	A-I-G	A-I-T	A-I-A		A-E-G	A-E-T		A-E-A

placed on the solid in the horizontal position. Then, the solid specimen was rotated until the drop was just about to roll down the solid surface. Figure 1 depicts the drop at this point. A measurement was then made of the advancing and receding angles by means of a coordinate cathetometer with a protractor eyepiece on the telemicroscope.\* The specimens were contained within a temperature controlled cabinet maintained at a temperature of 27°C and a relative humidity of approximately 70%. A tilting micro-manipulator# was used to tilt the specimens, as shown in Figure 5.

The liquids used were double distilled water, reagent grade iodobenzene<sup>+</sup> and absolute ethanol//. Solids on which the liquids were placed were acrylic resin<sup>≠</sup>, Teflon<sup>≠</sup>, polished glass cleaned with dichromate solution<sup>≠≠</sup>, silicone treated glass<sup>ϕ</sup>, wax treated glass<sup>∇</sup>, dental silicate cement<sup>≡</sup>, dental acrylic cement<sup>ω</sup>, dental amalgam<sup>Ω</sup> and a phenyl glycine-glycidyl methacrylic resin<sup>∞</sup>. Specimens of the dental materials were prepared according to their manufacturer's instructions.

---

\* Model 1238-1818 Cathetometer, Gaertner Scientific Corp, Chicago, Ill.

# Tilting micro-manipulator, Sobotka Inc., New York, N. Y.

+ Iodobenzene, Eastman Organic Chemicals, Rochester, New York.

// Absolute ethyl alcohol, reagent quality, U.S. Industrial Chemicals Co., New York, N. Y.

≠ Extruded acrylic sheet and Teflon sheet, Cadallic Plastics Co., Detroit, Mich.

≠≠ Polished Pyrex plate glass, Fred S. Hickey Corp, Schiller Park, Ill.

ϕ Desicote Silicone Coating, Beckman Instrument Co., California.

∇ Vista Wax, Simoniz Co., Chicago, Ill.

≡ Filling Porcelain (silicate cement), Batch #0306173 S. S. White Co., Philadelphia, Pa.

Ω True Dentalloy (amalgam alloy), Batch #18662353 S. S. White Co., Philadelphia, Pa.

ω Bonfil (acrylic resin), Batch #26350, L. D. Caulk Co., Milford, Del.

∞ Addent (phenyl glycine-glycidyl methacrylate resin), Minnesota Mining & Mfg. Co., St. Paul, Minn.

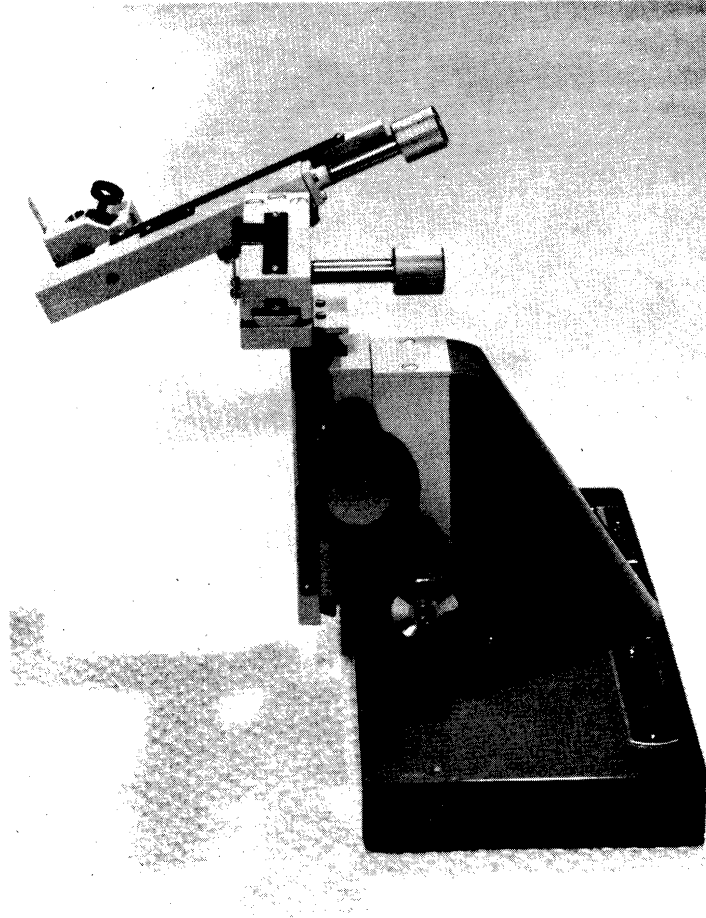


Figure 5. Micromanipulator Used for Contact Angle Measurements.

2. Surface Tension: The ring method was used to determine the surface tensions of the liquids. This method has been widely employed and involves the measurement of the force to detach a platinum ring from the surface of the liquid by means of a torsion balance.\*\* The instrument was calibrated with absolute ethyl alcohol.

3. Capillary Rise: The hyperbola method<sup>(14)</sup> was used to measure capillary rise. Two plates each 10 cm. by 14 cm. were clamped together so as to make a small angle with each other by inserting a shim between them at one end. Shims with thicknesses of 0.5, 0.75 and 1.0 mm. were used. The plates were secured in position by three rubber bands and held in a vertical position by means of a ringstand clamp. The combinations of materials and liquids used are shown in Table 1. In order to improve the flatness of the Teflon plates, they were bonded to plate glass by means of an epoxy adhesive.

The assembly of two plates separated at one edge by means of a shim, was lowered into the liquid. The constant temperature cabinet was then closed and the system allowed to come to equilibrium. The aforementioned coordinate cathetometer was used to measure the vertical height of the capillary curve from the vertex to the shim.

4. Surface Profile: In order to obtain an evaluation of the surface finish of the glass, acrylic, and Teflon plates, tracings of the surfaces were made. An electronic surface analyzer was used to obtain these recordings<sup>###</sup>. This device is shown in Figure 6.

---

\*\* Surface tension balance, Model #1396, A. Kruss Co., Hamburg.

### Microcorder model RLC, Micrometrical Div., Bendix Corp., Ann Arbor, Michigan.



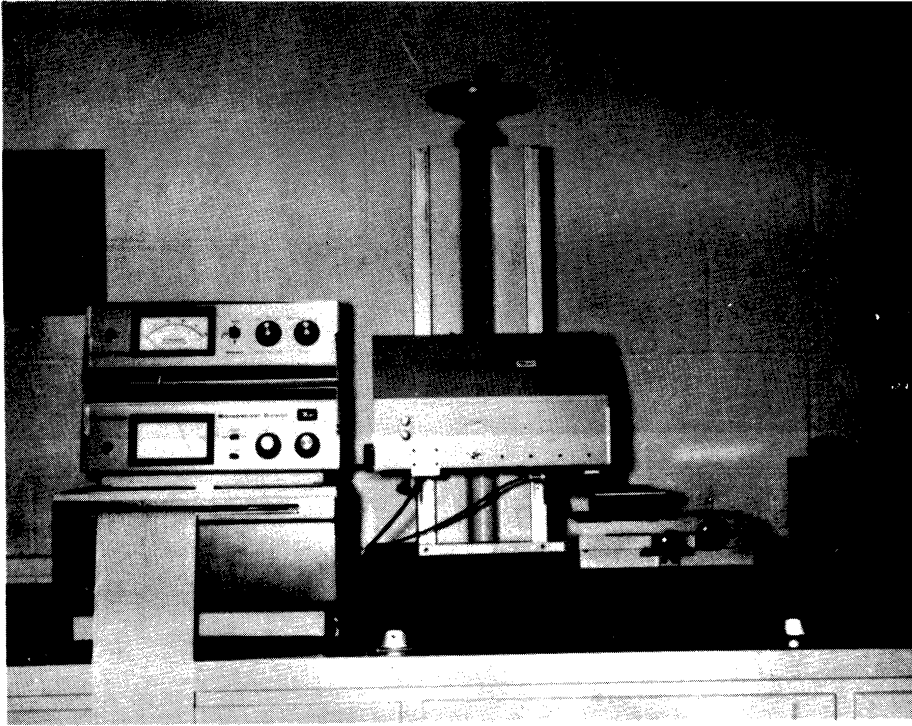


Figure 6. Surface Finish Analyzer.

C. Radioisotope Penetration Study

Sound incisor, molar, bicuspid, and cuspid teeth were extracted and stored in a dilute solution of hydrogen peroxide. Type V cavity preparations were formed in these teeth. Three treatments were applied with ten replications per treatment group. Figure 7 shows the three treatments employed. The teeth in treatment group 1 were filled with powdered dental inlay wax.\* The surface of the compacted filling were smoothed over with a hot spatula. Treatment 2 consisted of coating the walls of the preparation from the cavo-surface angle to the cavity base with melted inlay wax. The prepared cavities were then filled with powdered inlay wax and finished with a hot spatula. Treatment 3 was similar to treatment 2 in the coating of the cavity walls. However, in this treatment, the floors of the cavities were coated with melted wax. As in treatment 1 and 2, the cavities were filled with powdered wax and finished with a hot spatula.

In all three treatments, a small piece of cotton thread was placed at the center of the cavity floor after the coating of the walls and floors had been completed, but before the powdered wax fillings had been placed.

The filled teeth were placed into a vial containing a dilute aqueous solution of sodium radiocarbonate,  $\text{Na}_2^{14}\text{CO}_3$ , as shown in Figure 8. This solution# contained approximately 1 microcurie per milliliter of  $^{14}\text{C}$ . In order to minimize penetration through the roots, the teeth were placed in the solution so that the apical portions were above the liquid level. Sticky wax on the floor of the vials was used to maintain this orientation. The teeth were left in this radioactive solution for 24 hours. At the end of that period, the teeth were

\* Kerr's Blue Inlay Wax, Control #0141B806, Kerr Mfg. Co., Detroit, Mich.  
# Carbon - 14 Solution, SL-71-1, Atomic Accessories Co., Valley Stream, N.Y.

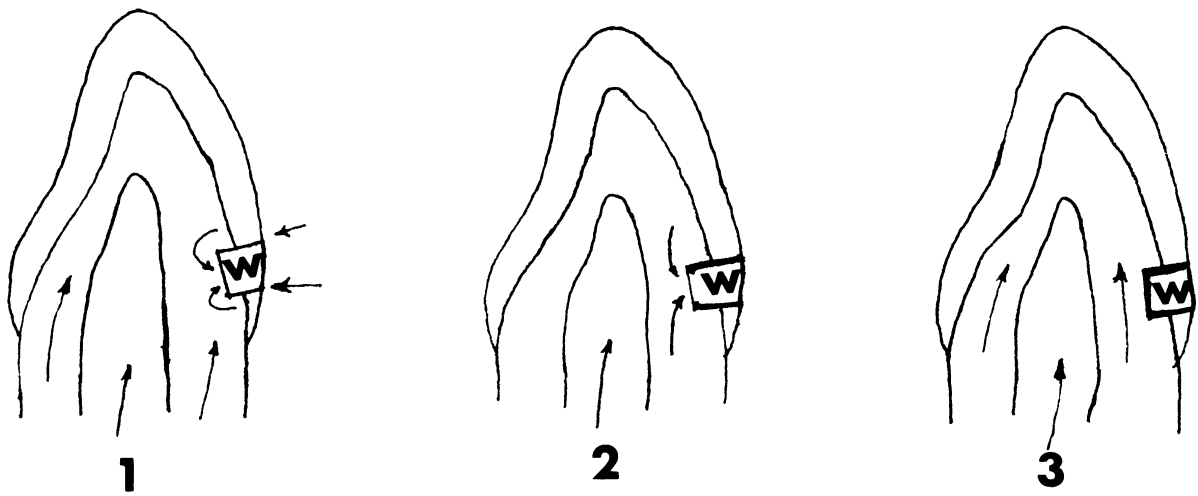


Figure 7. Treatments Applied to Extracted Teeth: 1. Wax Filling; 2. Wax Coating of Walls With Opening on Base and With Wax Fillings; 3. Complete Wax Coating of Cavity Surface and Wax Filling.



Figure 8. Tooth Immersed in Radioactive Solution for Penetration Tests.

rinsed off with tap water and the cotton strings were recovered by removing the wax fillings. Upon recovering the absorbent threads, they were placed in sample vials for radioactivity counting. Liquid scintillation counting was the method chosen for measuring the amount of radioactive carbon absorbed by the threads.  $^{14}\text{C}$  decays by negatron emission to  $^{14}\text{N}$ . The negatron emitted has an energy of 0.155 Mev. The liquid scintillation solution used consisted of the following: a solvent (dioxane and naphthalene), a primary fluor (2,5 - diphenyloxazole) and a secondary fluor (2,2 - paraphenylene bis 5 - phenyloxazole). It is the primary fluor which converts the beta particle energy to light energy. The secondary fluor is used to shift the wave-length of the light emitted by the primary fluor to a longer wavelength to which the photomultiplier tube is more sensitive.

The vials containing the threads and a measured amount of scintillation solution were placed in the deep-freeze counting chamber.\* During counting, the vials were brought within range of a photomultiplier tube which converts the light energy into electronic signals of sufficient strength so that they could be measured. Both the detector solution and the photomultiplier were placed in a deep freeze unit to minimize random electronic pulses. The number of background pulses was diminished by following this procedure. Each sample was counted for a period of ten minutes. The counting unit is shown in Figure 9.

---

\* Tri-Carb Liquid Scintillation Spectrometer, model 314, Packard Instrument Co., Downers Grove, Ill.

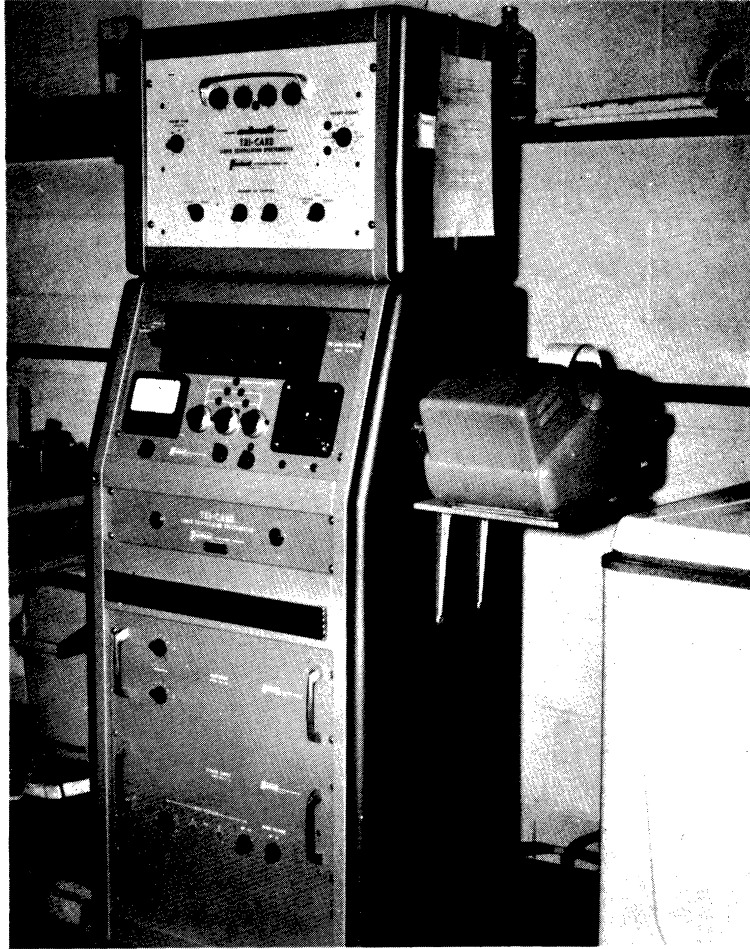


Figure 9. Liquid Scintillation Spectrometer.

## V. EXPERIMENTAL RESULTS

### A. Parameters

1. Contact Angles: The advancing and receding contact angles along with the number of replications,  $n$ , are given in Table 2. The values for water on acrylic agree with those of Craig, Berry, and Peyton. The mean values for water on Teflon are slightly lower, but within reasonable agreement with the values reported by Kawasaki.<sup>(3)</sup> Silicone coated glass exhibited an advancing contact angle value of  $91^\circ$ . As shown, the contact angle values of ethanol and iodobenzene are considerably lower than those of water on the same solids. Iodobenzene exhibited poorer wetting on glass than might be expected of an organic liquid. However, this may be explained on the basis of the lack of ability of iodobenzene molecules to penetrate adsorbed organic monolayers. Ethanol, in contrast, spreads completely on glass due to its penetrating and solvent action. The commercial dental materials tested showed contact angles less than  $90^\circ$  with water. Of the dental filling materials, amalgam, which had set for 24 hours, gave the highest angle of contact with water. The mixing proportions of mercury to allow was 8 to 5. The pooled standard deviation was calculated to be 6 degrees for these measurements.

2. Surface Tension: The surface tensions of ethanol, iodobenzene, and distilled water were found to be 22.3, 39.1 and 70.9 dynes per centimeter at  $27^\circ\text{C}$ . Values reported in the literature<sup>(34)</sup> were 22.3, 39.7 and 71.6 dynes per centimeter.

3. Capillary Rise: The capillary rise,  $h$ , was measured at several distances,  $x$ , from the vertex of the plates for the permutations given in the factorial table. The data are represented graphically

TABLE 2  
 CONTACT ANGLES OF LIQUIDS ON  
 VARIOUS SOLIDS AT 27°C.

Solid	Liquid	$\theta_A$ Degrees	$\theta_R$ Degrees	n
Acrylic	Water	74	54	5
Teflon	Water	110	82	4
Glass	Water	14	11	6
Desicote	Water	91	65	6
Acrylic	Ethanol	Spreads		3
Teflon	Ethanol	29	16	7
Glass	Ethanol	Spreads		3
Acrylic	Iodobenzene	20	12	7
Teflon	Iodobenzene	59	31	3
True Dentalloy	Water	77	65	5
Filling Porcelain	Water	12	6	3
Bonfil	Water	38	35	3
Addent	Water	51	39	5
Vista	Water	53	42	3



as rise-distance curves. The curves for the water systems are contained in Figures 10 to 19. Each data point represents the height of the liquid above the liquid level in the trough. Curves representing the rise obtained with three different combinations of plates are presented in Figure 10. The rise curve obtained when two glass plates were used is the highest of the three. When a silicone treated plate was substituted for one of the glass plates, the capillary rise was reduced to approximately one half that obtained with the two glass plates. Substitution of a Teflon plate produced the data for curve "c" in Figure 10. This curve shows the lowest capillary rise of the three in Figure 10. The capillary rise curves for the systems using ethanol are found in Figures 20 to 25 and those for iodobenzene systems are found in Figures 26 to 30. The average  $x_h$  value for each curve and the angle between the plates are given in the legend of each figure. These data will be analyzed statistically in the next section.

4. Surface Profile: Recordings of the surface profiles of the glass, acrylic and Teflon plates used in the capillary rise experiments are shown in Figure 31. All three profile curves were obtained at the same amplification.

#### B. Radioisotope Penetration Results

In Table 3 are given the results of the radioactivity counting on the cotton strings for the three treatments and the background. An analysis of variance test was made to determine the significance of the treatment differences with respect to the error variance. The results of this analysis are given in Table 4. Since the F value obtained exceeded the critical F value of 2.90 at the 0.05 level, the treatments

TABLE 3  
RADIOACTIVITY COUNTS PER TEN MINUTES  
FOR TREATMENTS OF EXTRACTED TEETH

	Treatments			
	1	2	3	4
	237	550	163	178
	1320	404	197	160
	384	308	155	189
	3287	368	194	209
	302	372	174	193
	261	977	179	154
	286	411	150	194
	181	286	169	160
	279	271	283	168
	255	300	193	111
$\bar{x}$	679	424	186	172

TABLE 4  
ANALYSIS OF VARIANCES FOR RADIOACTIVITY  
COUNTS FOR DIFFERENT TREATMENTS

Source of Variance	Sums of Squares	Degrees of Freedom	Mean Square	F
Treatments	2,164,203	3	721,401	3.05
Error	8,537,437	36	236,873	
Total	10,691,640	39		

TABLE 5  
RESULTS OF DUNCAN'S NEW MULTIPLE RANGE  
TEST FOR RADIOACTIVITY DIFFERENCES

Treatments	Difference	LSR	Significant
4 - 1	507	477	Yes
4 - 2	352	464	No
3 - 1	493	464	Yes
3 - 2	238	440	No
2 - 1	255	440	No

produced a significant difference in average radioactivity. In order to rank the treatments in the amount of radioactivity produced, Duncan's new multiple range test was employed.<sup>(35)</sup> The problem was to determine which of the differences among the four mean counts were significant. The results of this test are given in Table 5. Here "LSR" represents the least significant ranges. If the difference between the means being compared exceeded the LSR value, a significant difference was indicated.

A modified Student's  $t$  test was employed to test for a significant difference between treatment 2 and treatment 4, the background. The  $t$  value obtained was 3.71 with 18 degrees of freedom. Since the assumption that the variances of treatments 2 and 4 are equal cannot be made, the critical  $t$  value was found by entering the  $t$ -table at 9 degrees of freedom. This procedure gave a critical  $t$  of 3.25 at the 0.01 level. Therefore, this conservative test indicated a significant difference existed between treatments 2 and 4, although Duncan's test did not.

These tests indicate that leakage of liquid around a wax restoration without treatment of the tooth surface is significant. Second, even if the walls are treated with wax, penetration still occurs if the floor of the cavity is not sealed. And finally, no significant amount of penetration occurs if the entire cavity surface is coated with wax and a wax filling is placed. Discussion of these results will be given in a later section on application.

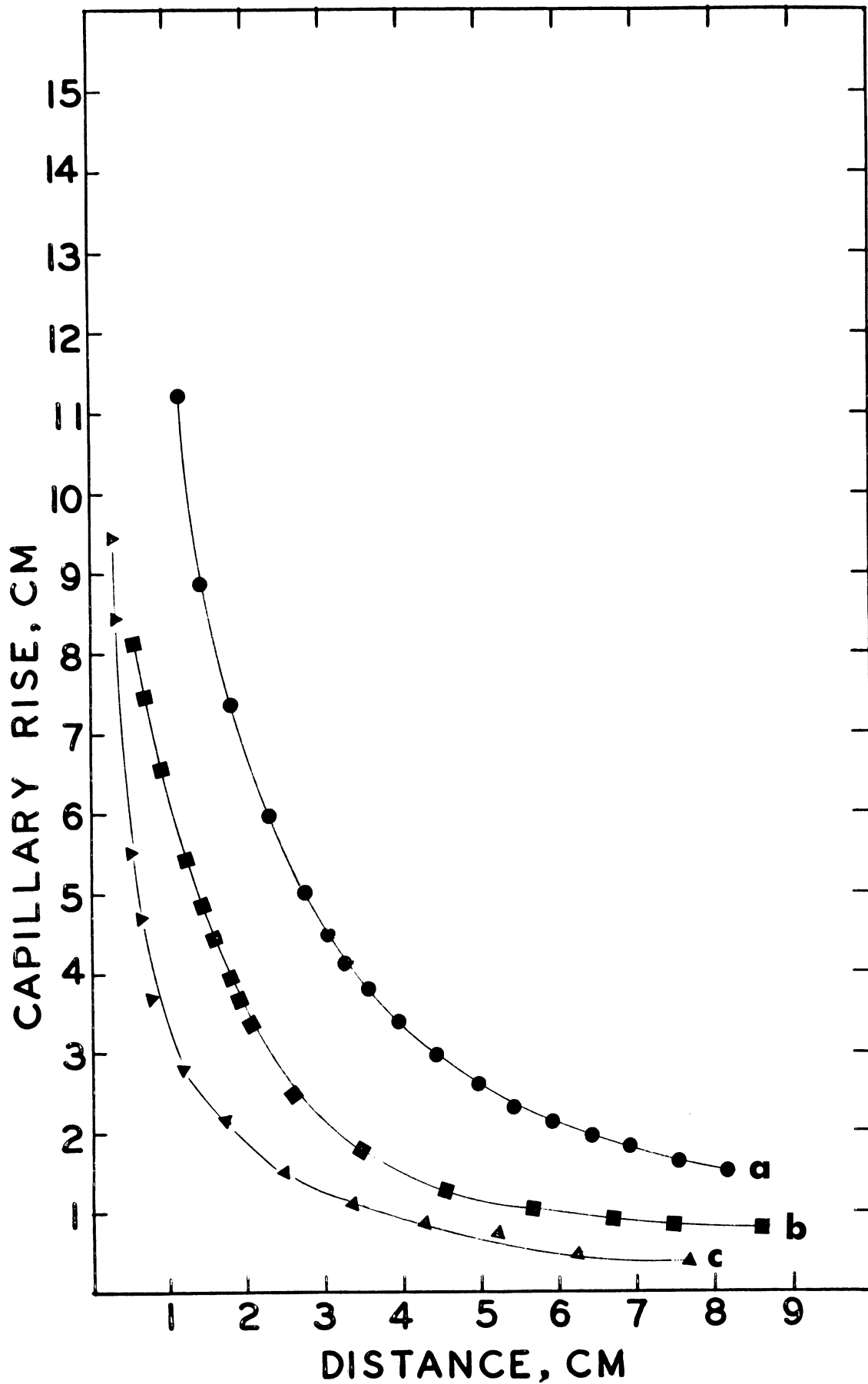


Figure 10. Capillary Rise Curves for: (a) Glass-Water-Glass,  $\bar{x}_h = 13.16$ ; (b) Silicone-Water-Glass,  $\bar{x}_h = 6.35$ ; (c) Teflon-Water-Glass,  $\bar{x}_h = 3.32$  sq. cm.  $\phi = 38'$ .

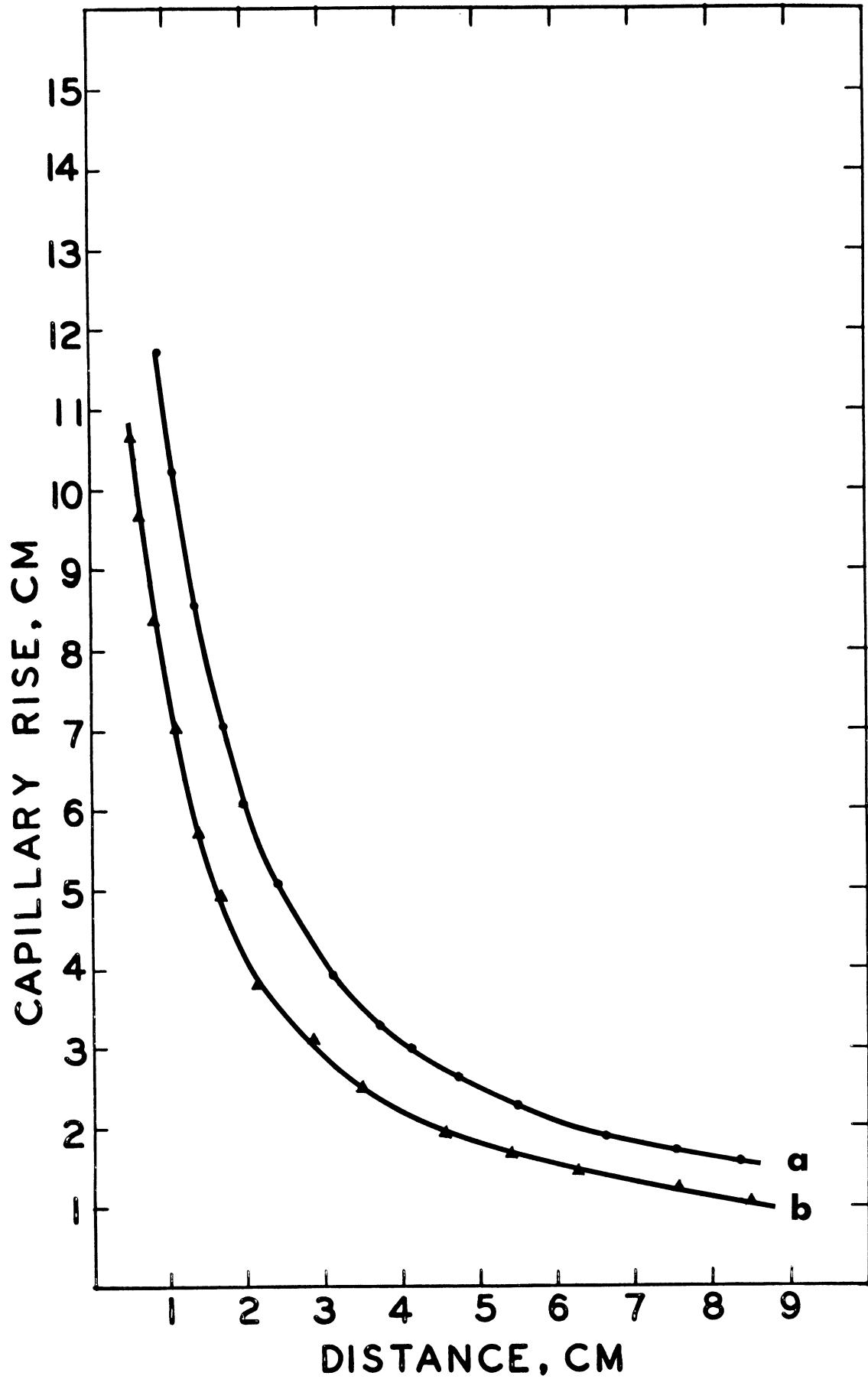


Figure 11. Capillary Rise Curves for: (a) Glass-Water-Glass,  $\bar{x}h = 12.36$ ; (b) Glass-Water-Acrylic,  $xh = 8.09$  sq. cm. Both With  $\phi = 38'$ .

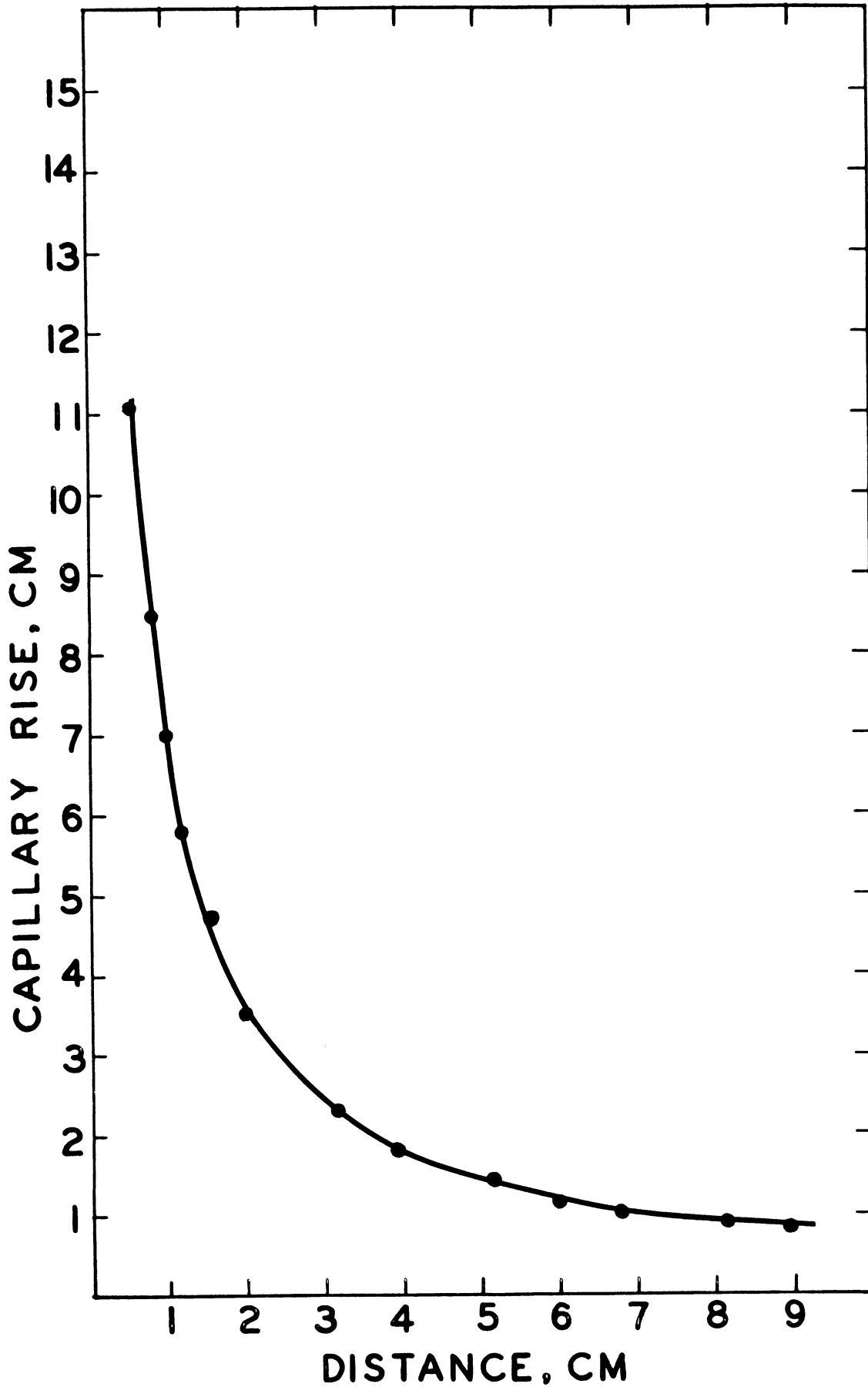


Figure 12. Capillary Rise Curve for Glass-Water-Silicone.  $\phi = 38'$ .  
 $\bar{x}h = 6.93$  sq. cm.



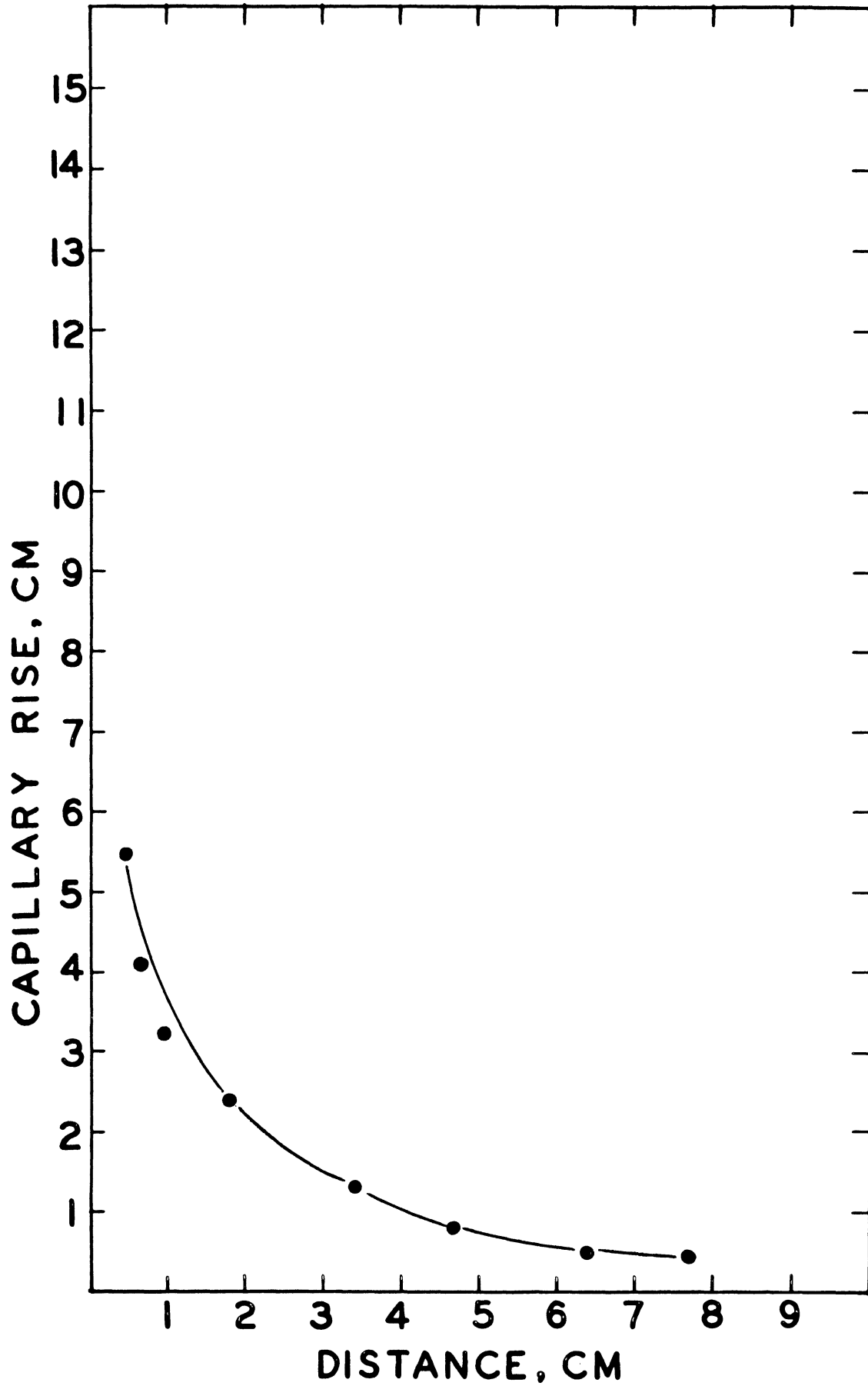


Figure 13. Capillary Rise Curve for Acrylic-Water-Acrylic.  $\phi = 38'$ .  
 $\bar{x}h = 3.44$  sq. cm.

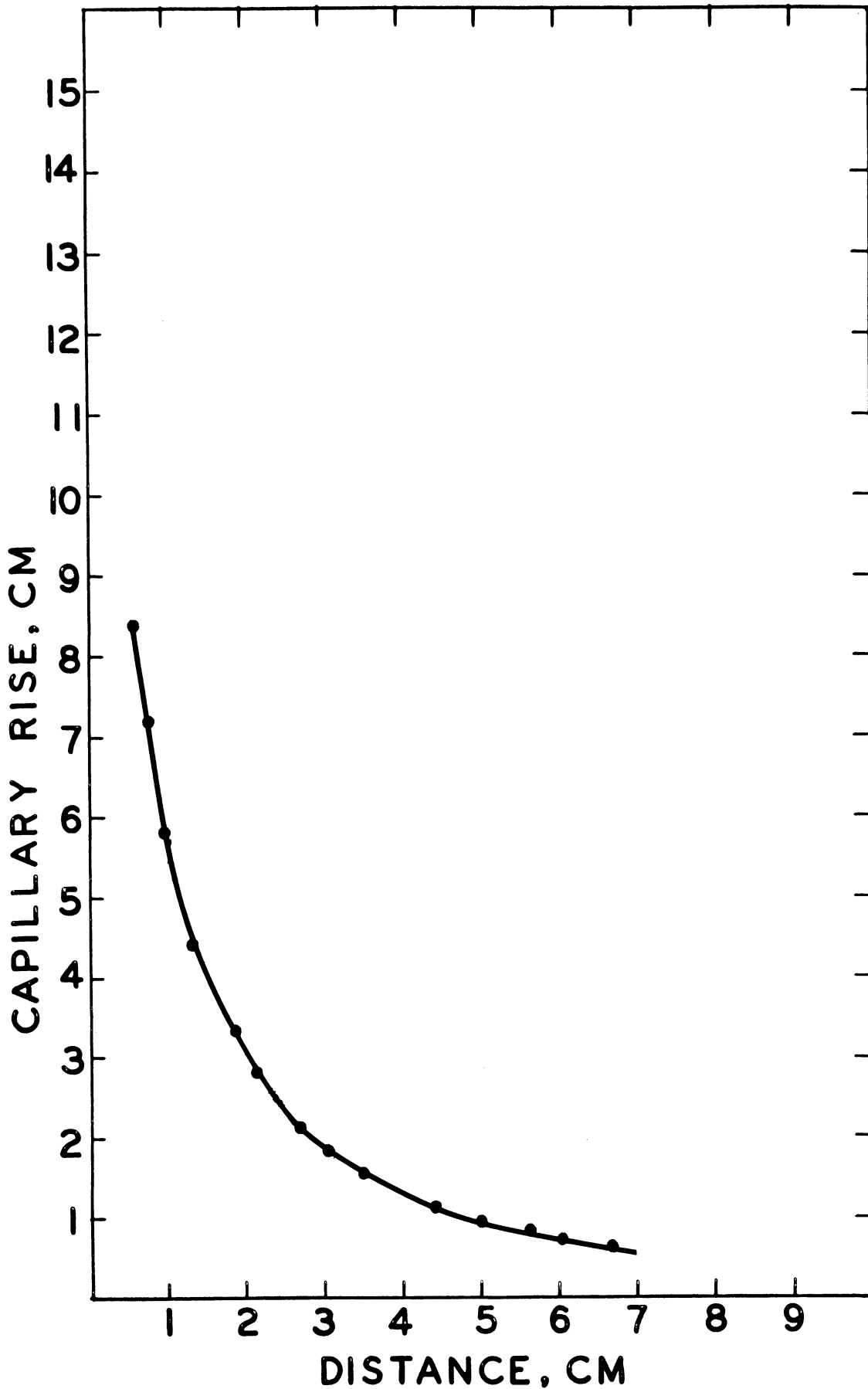


Figure 14. Capillary Rise Curve for Vista-Water-Vista.  $\phi = 42'$ .  
 $\bar{x}h = 6.90$  sq. cm.

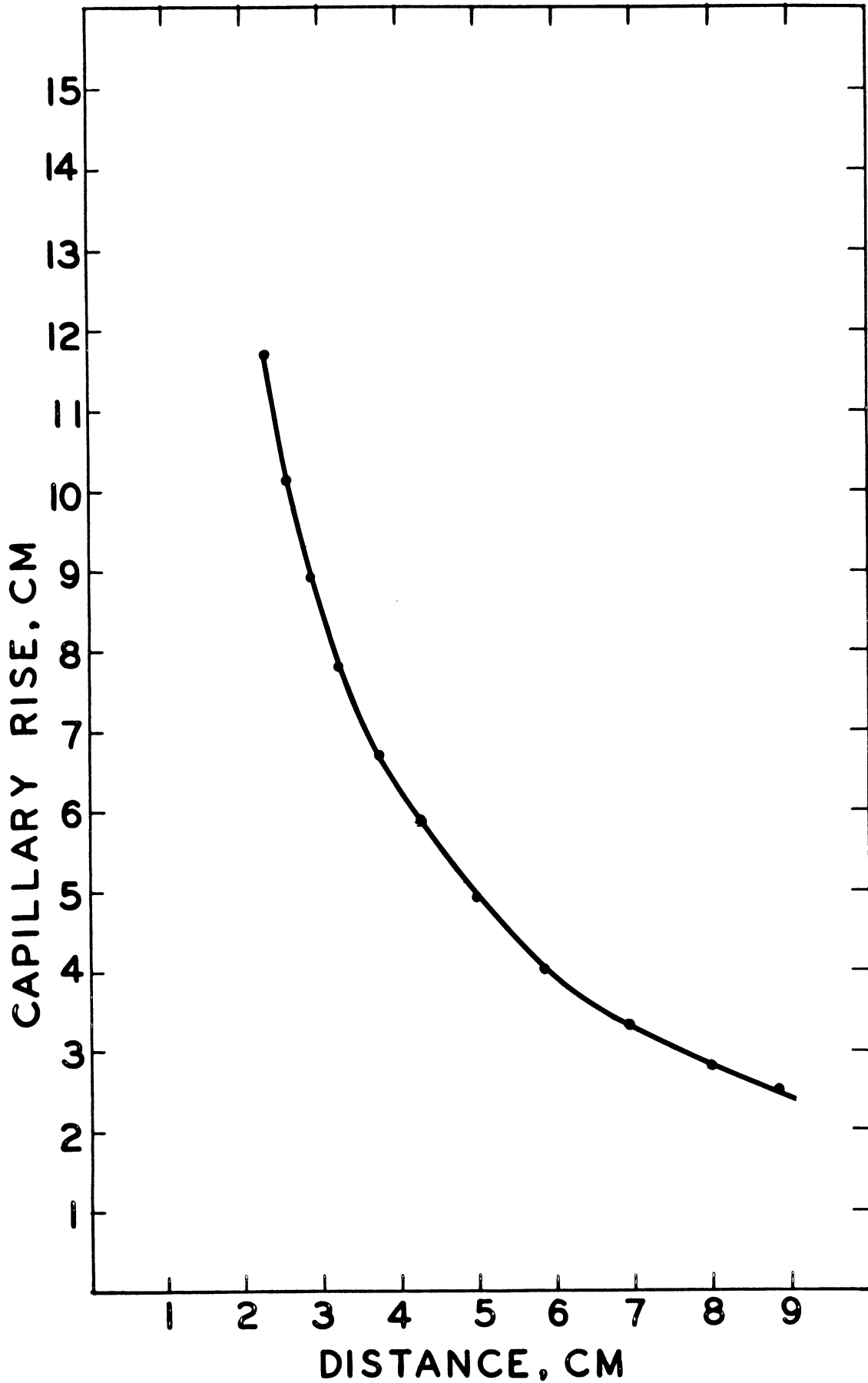


Figure 15. Capillary Rise Curve for Glass-Water-Glass.  $\phi = 18'$ .  
 $xh = 24.44$  sq. cm.

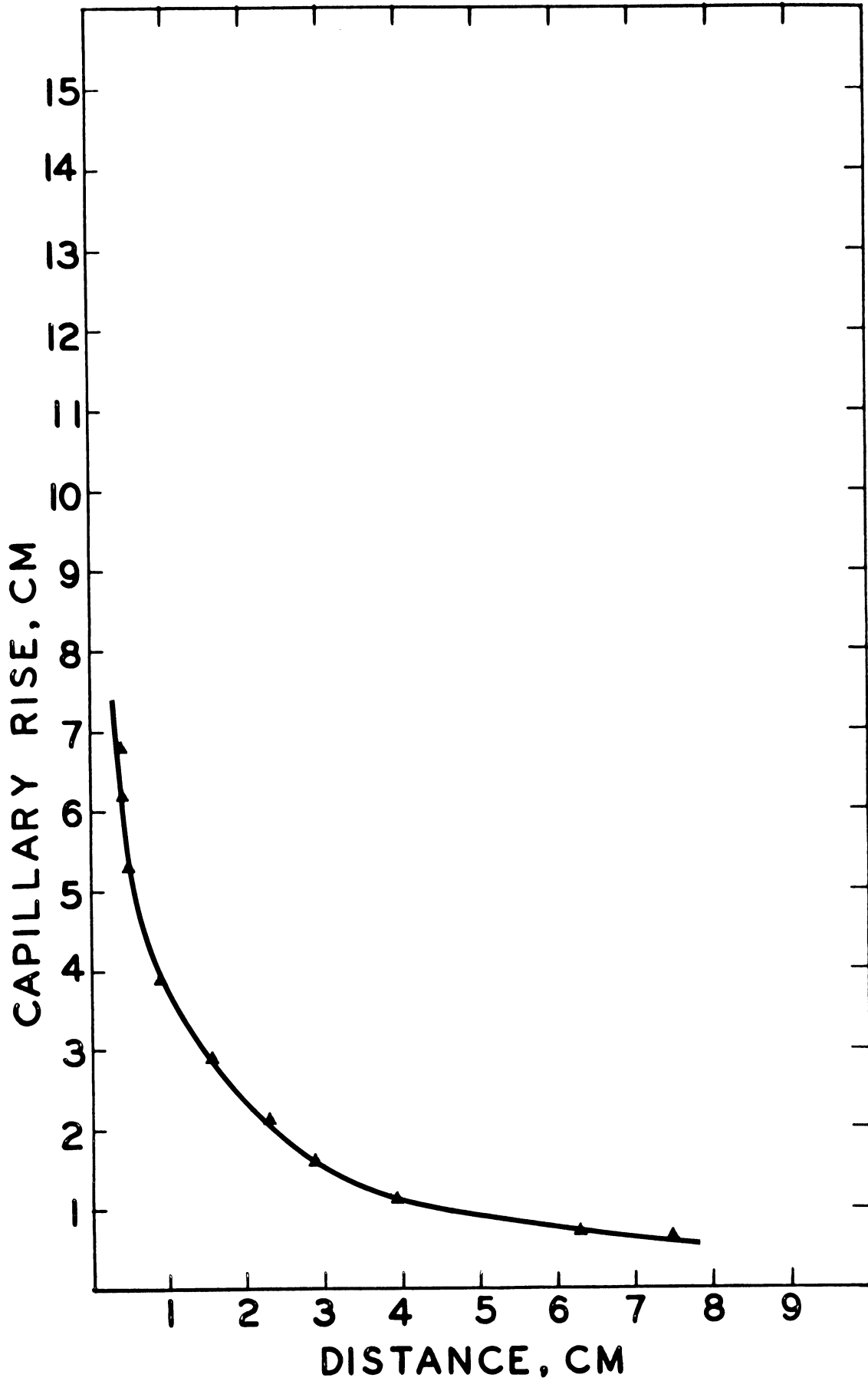


Figure 16. Capillary Rise Curve for Silicone-Water-Acrylic.  $\theta = 38'$ .  
 $\bar{x}h = 3.81$  sq. cm.

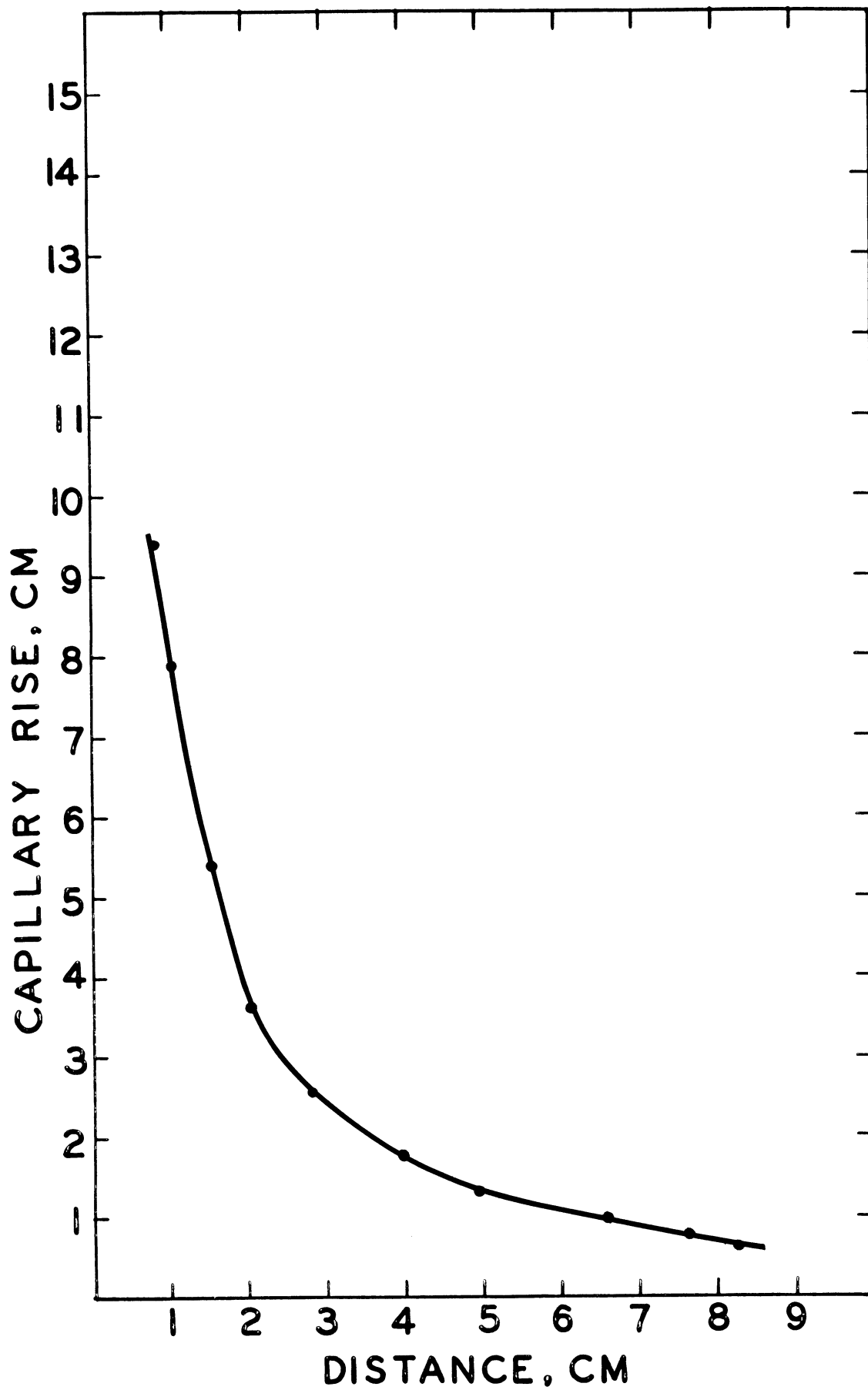


Figure 17. Capillary Rise Curve for Vista-Water-Vista.  $\phi = 42'$ .  
 $\bar{x}h = 6.94$  sq. cm.

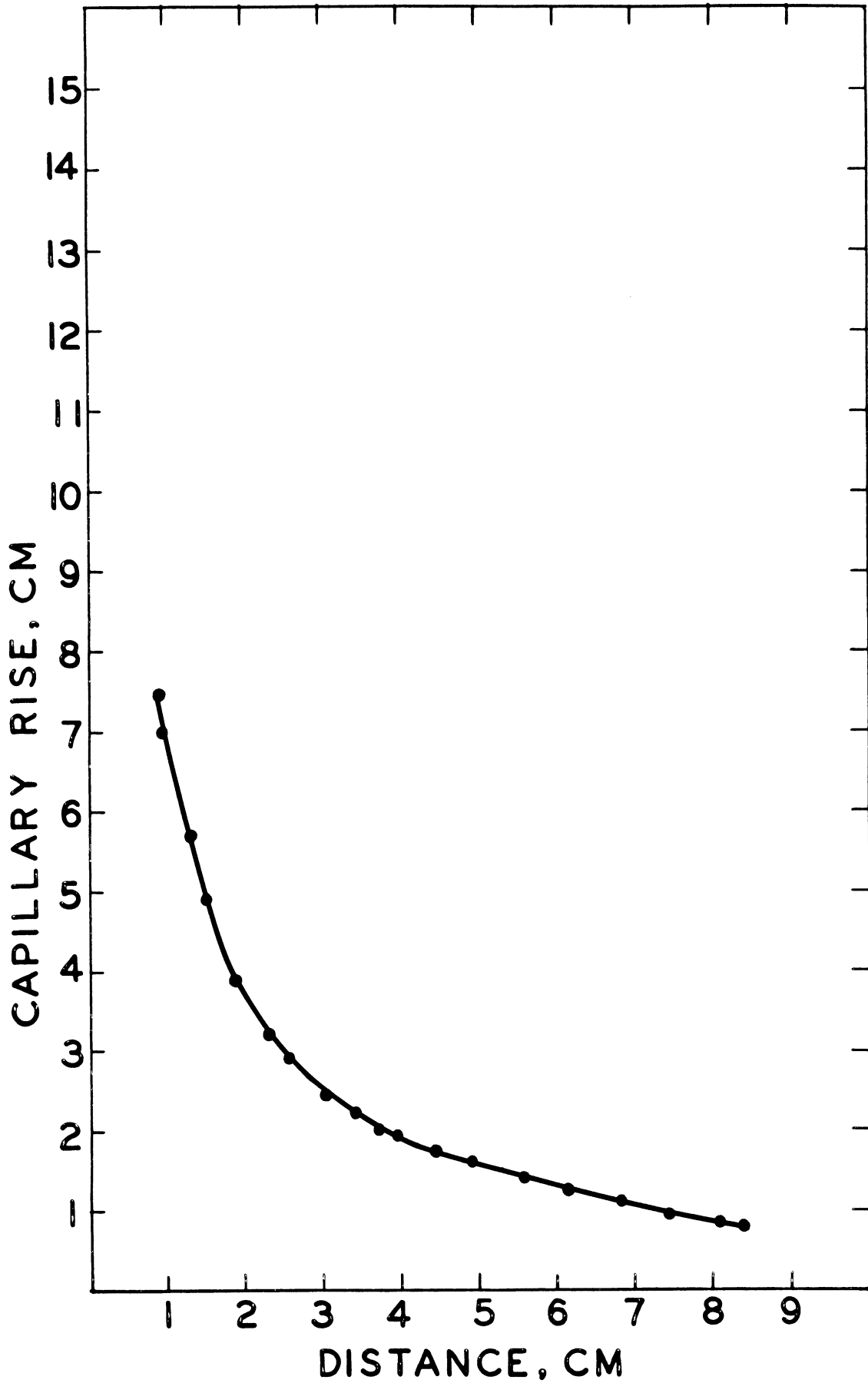


Figure 18. Capillary Rise Curve for Glass-Water-Acrylic.  $\phi = 38'$ .  
 $\bar{x}h = 7.34$  sq. cm.

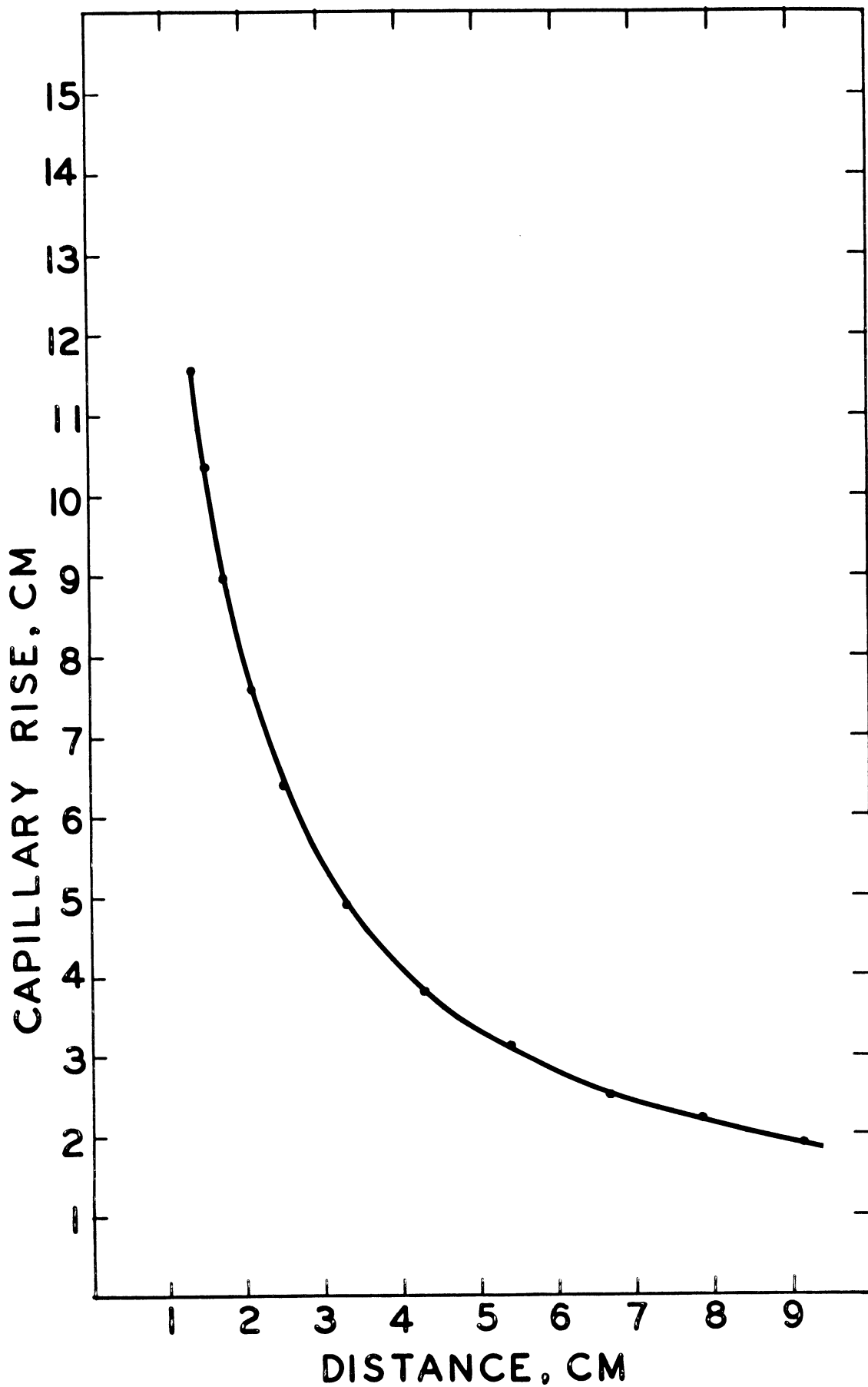


Figure 19. Capillary Rise Curve for Glass-Water-Glass.  $\phi = 26'$ .  
 $xh = 16.3$  sq. cm.

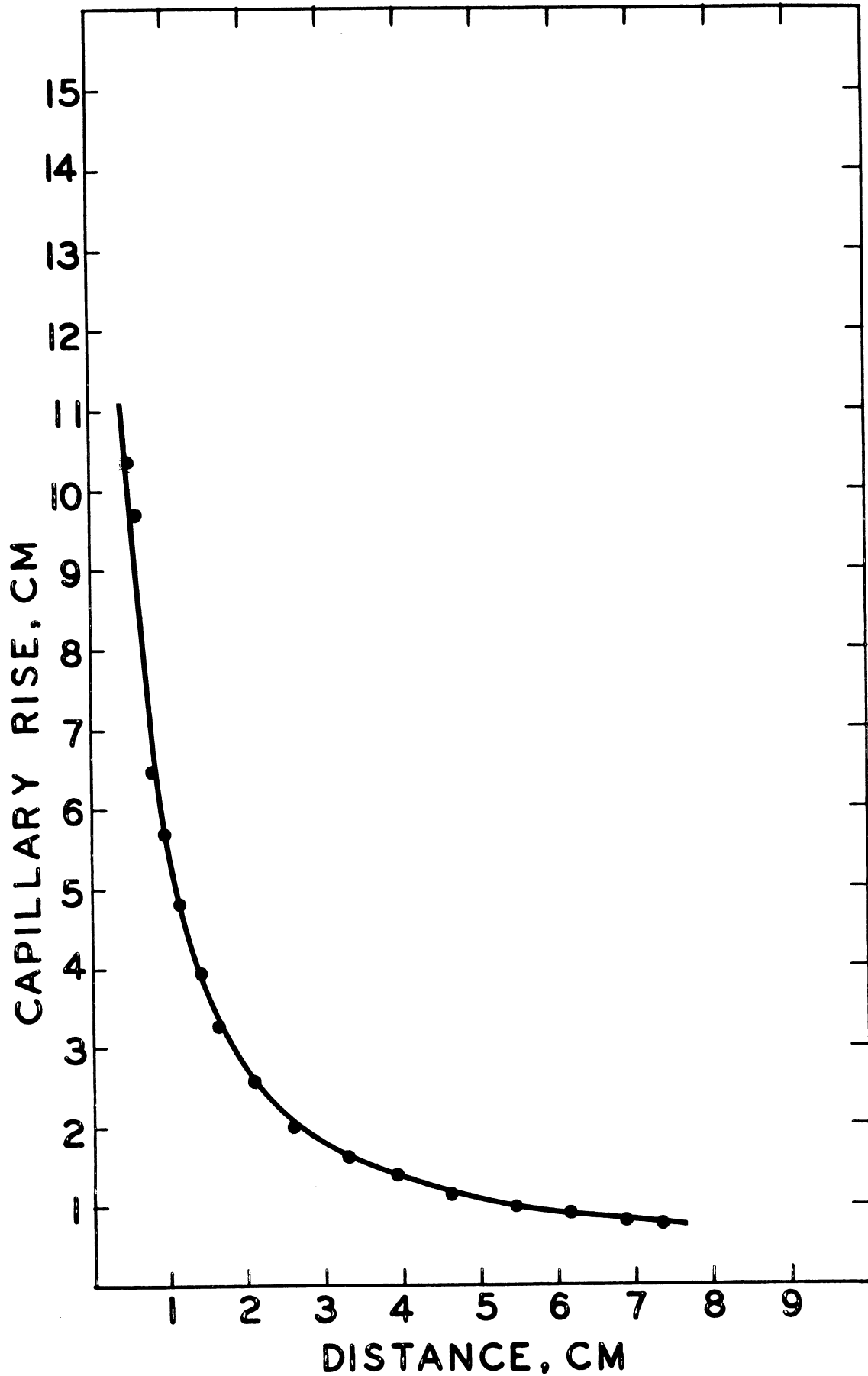


Figure 20. Capillary Rise Curve for Glass-Ethanol-Glass.  $\phi = 38'$ .  
 $\bar{x}h = 5.45$  sq. cm.



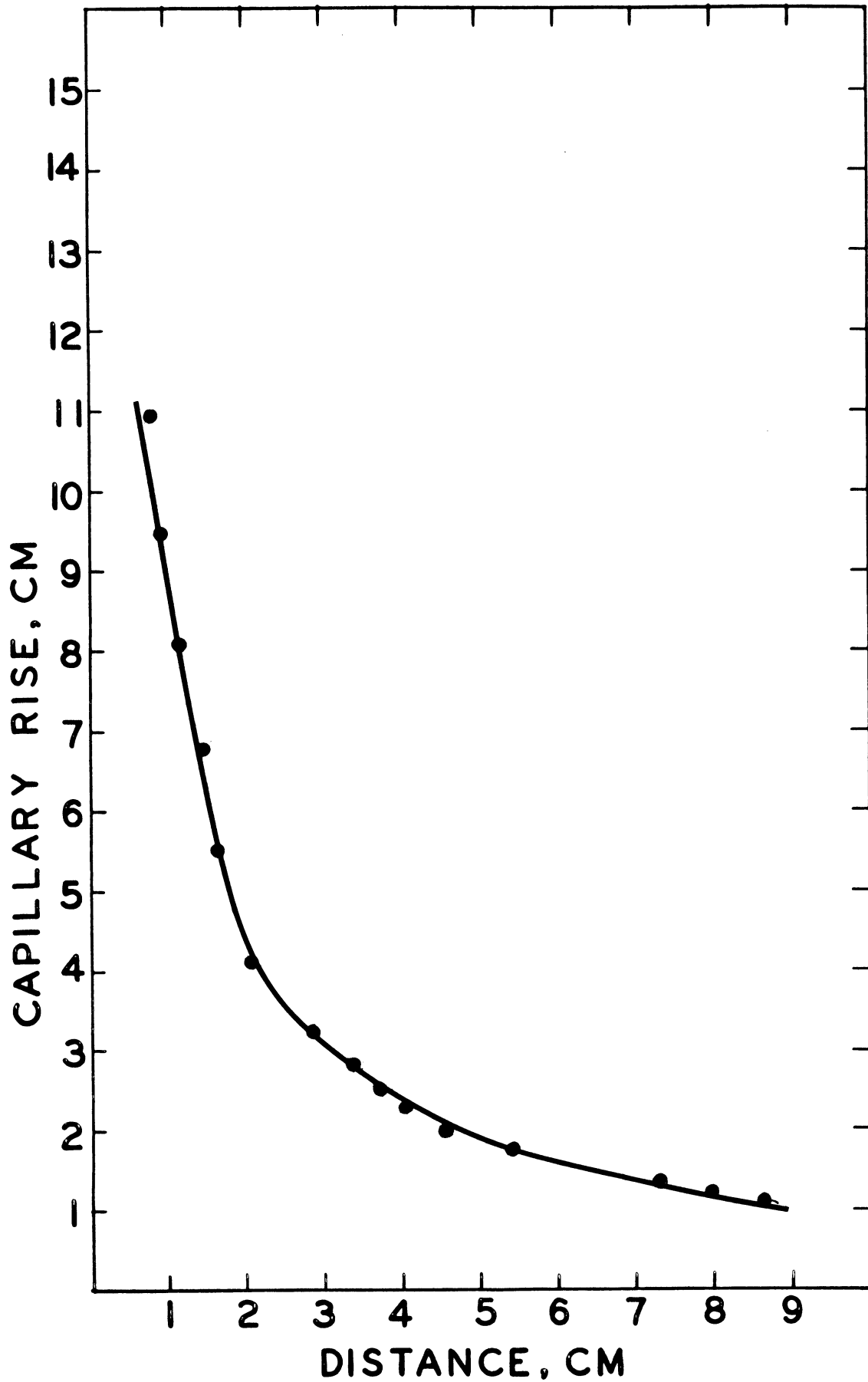


Figure 21. Capillary Rise Curve for Acrylic-Ethanol-Glass.  $\phi = 18'$ .  
 $\bar{x}h = 9.36$  sq. cm.

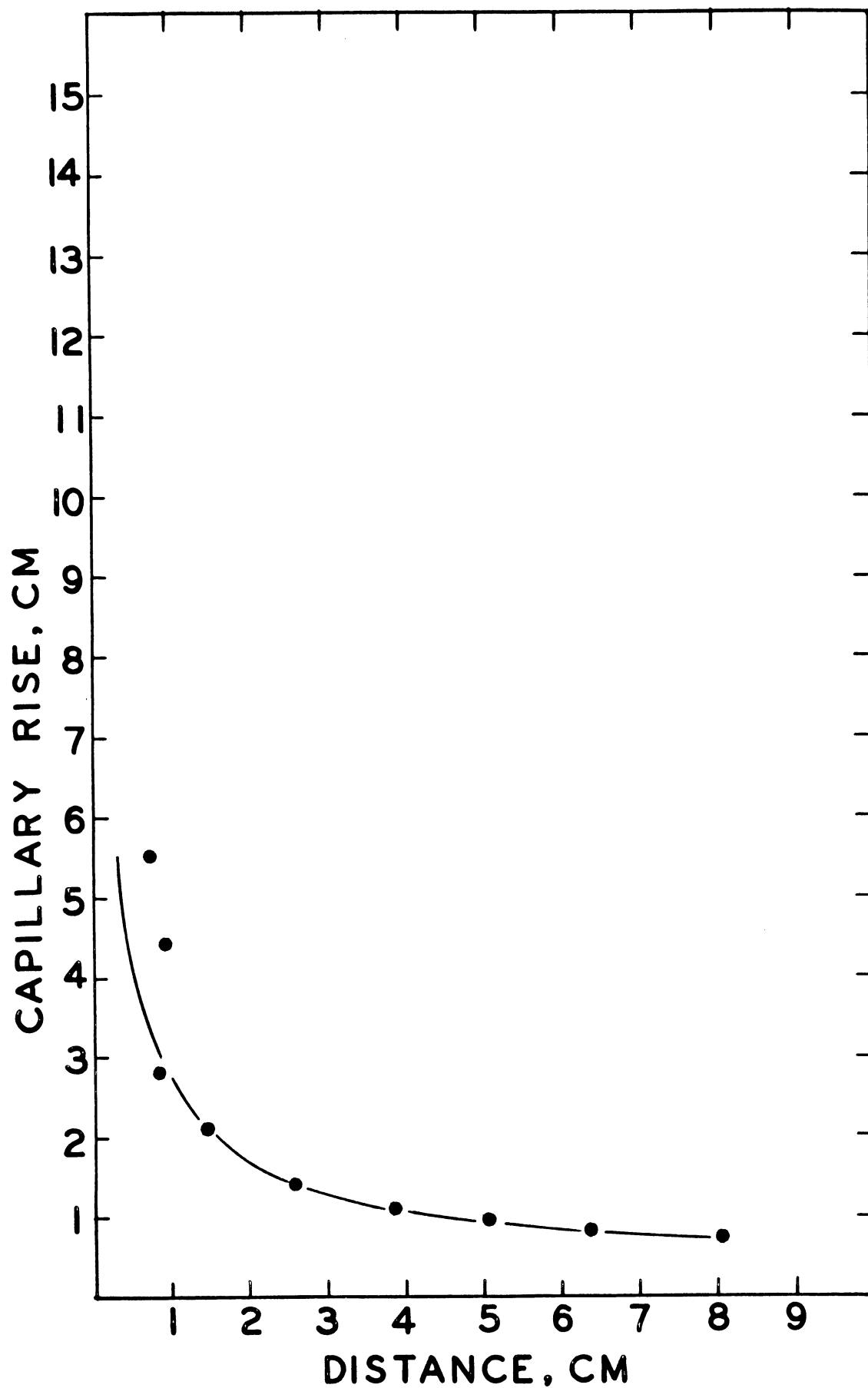


Figure 22. Capillary Rise Curve for Acrylic-Ethanol-Teflon.  
 $\phi = 38'$ .  $\bar{x}h = 4.18$  sq. cm.

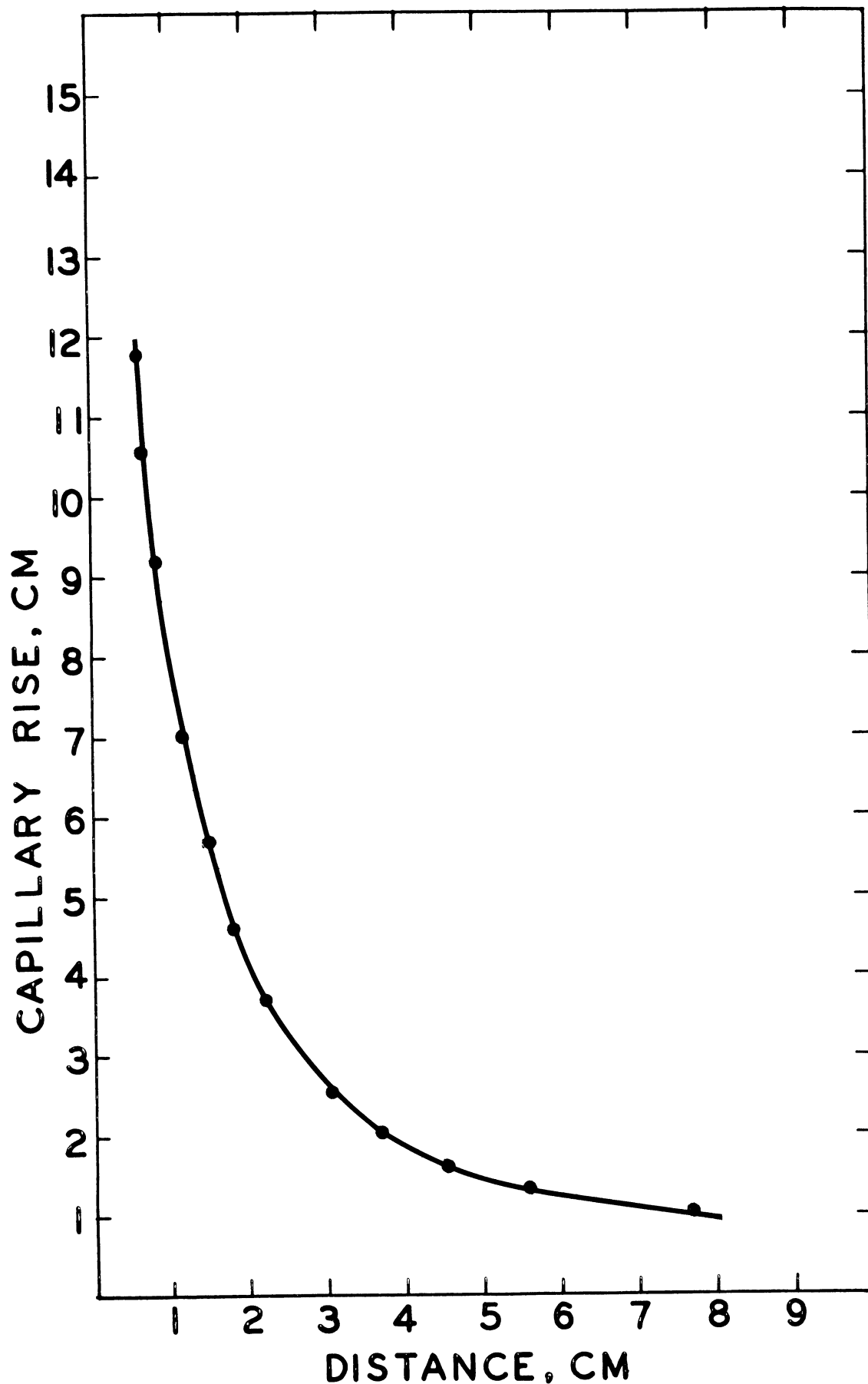


Figure 23. Capillary Rise Curve for Glass-Ethanol-Acrylic.  
 $\phi = 26'$ .  $\bar{x}h = 7.55$  sq cm.

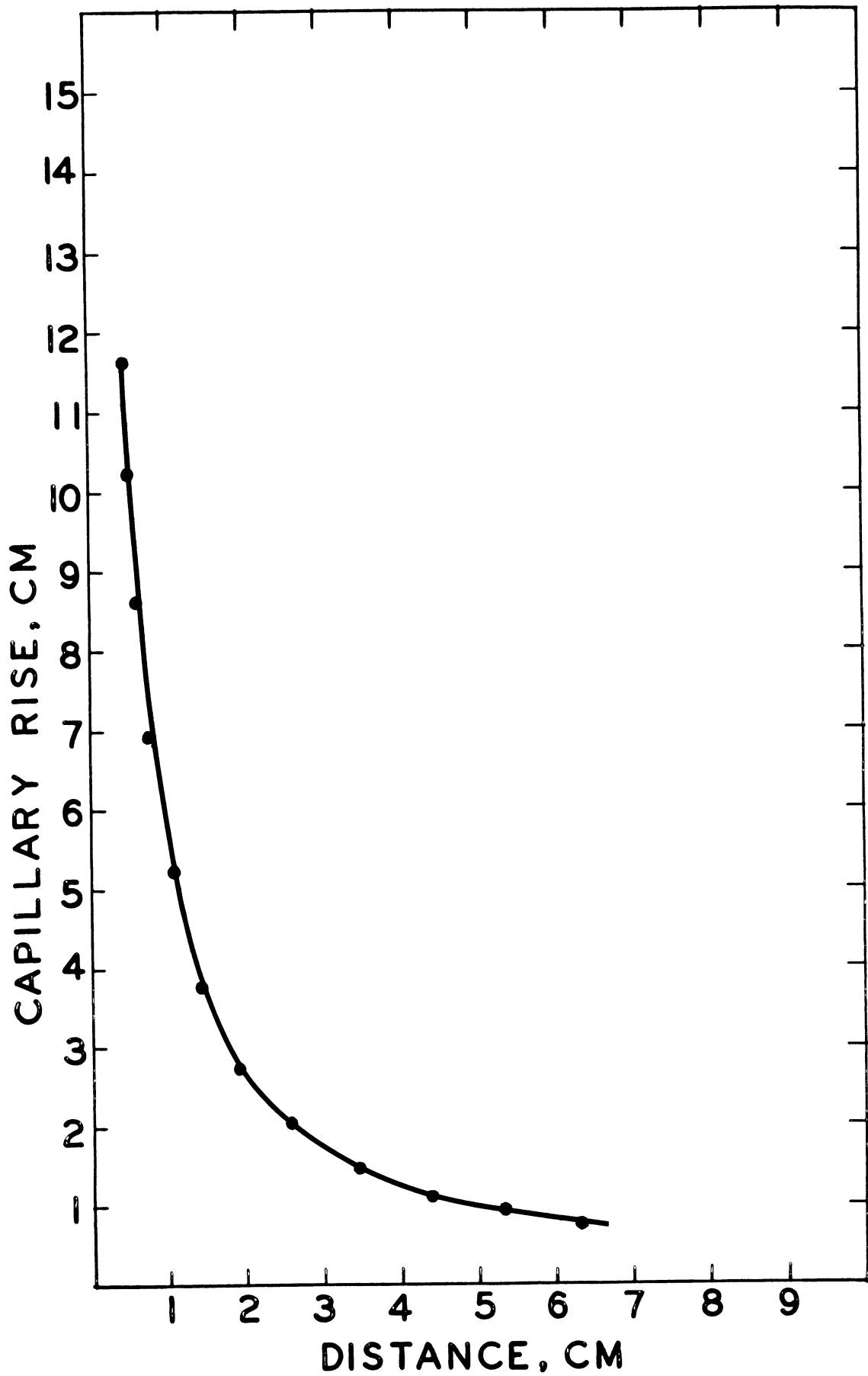


Figure 24. Capillary Rise Curve for Acrylic-Ethanol-Glass.  
 $\phi = 38'$ .  $\bar{x}h = 5.05$  sq. cm.

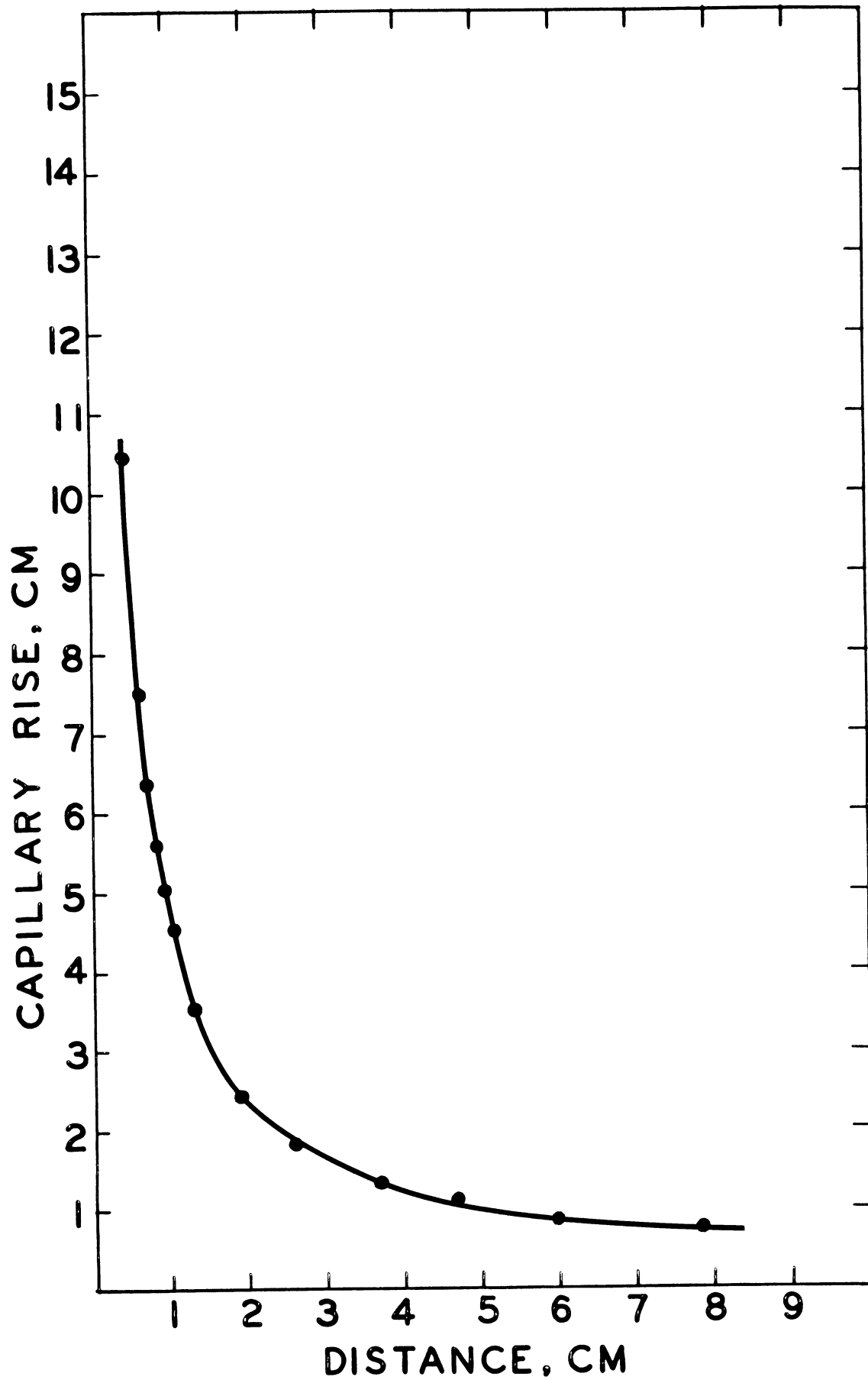


Figure 25. Capillary Rise Curve for Acrylic-Ethanol-Acrylic.  
 $\theta = 38'$ .  $xh = 4.8$  sq. cm.

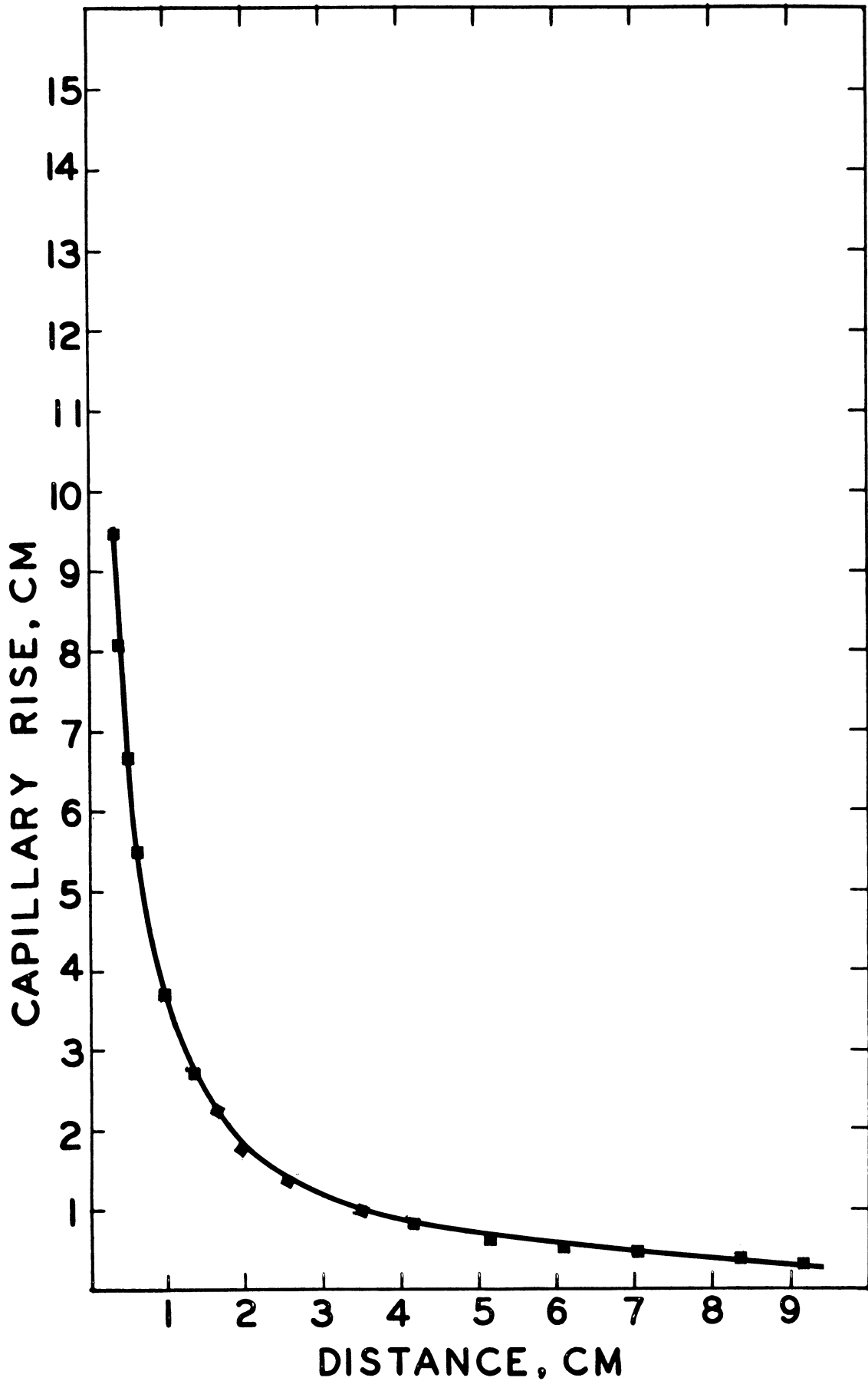


Figure 26. Capillary Rise Curve for Acrylic-Iodobenzene-Acrylic.  
 $\phi = 38'$ .  $xh = 3.32$  sq. cm.

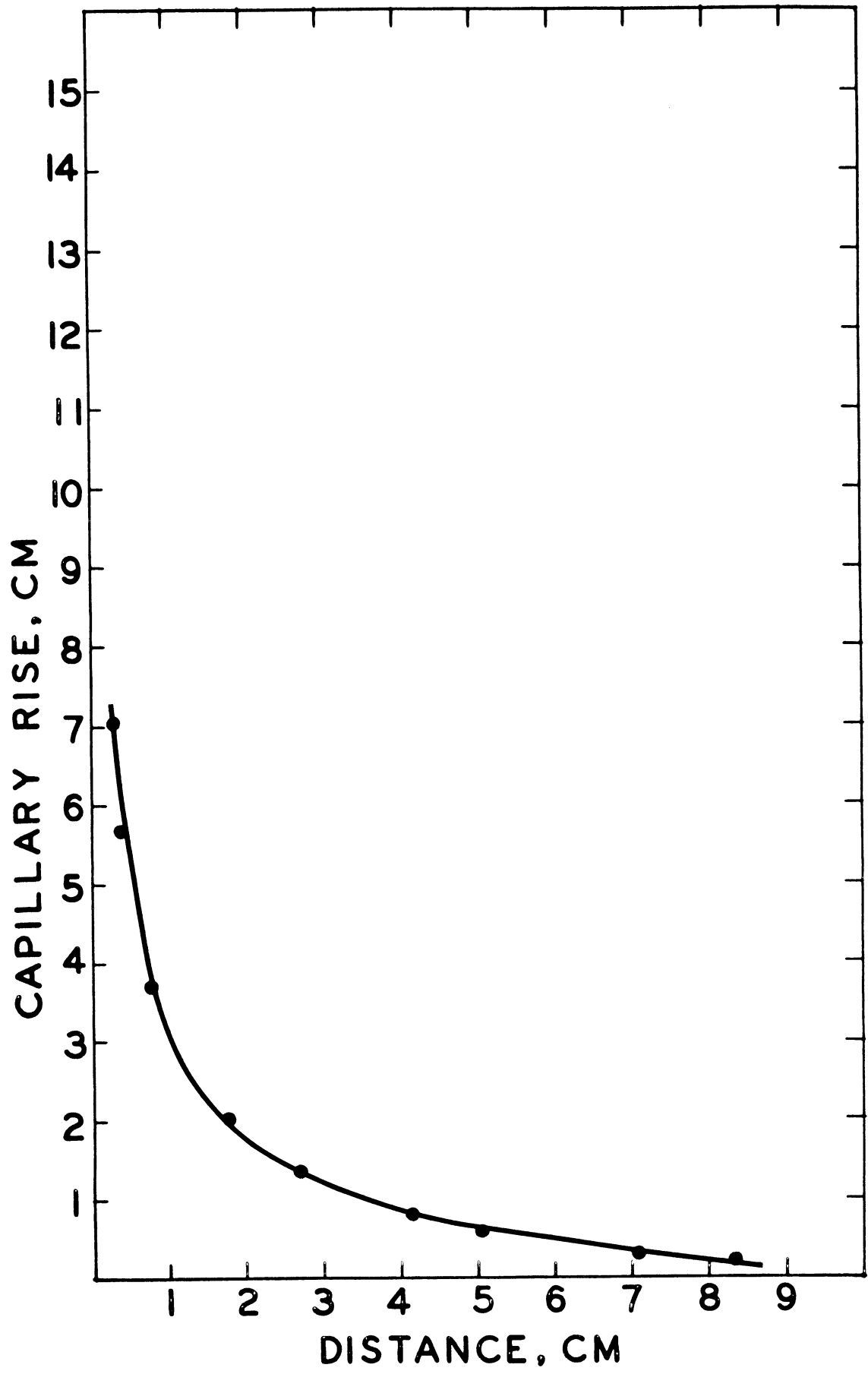


Figure 27. Capillary Rise Curve for Teflon-Iodobenzene-Acrylic.  
 $\phi = 38'$ .  $\bar{x}h = 2.82$  sq. cm.

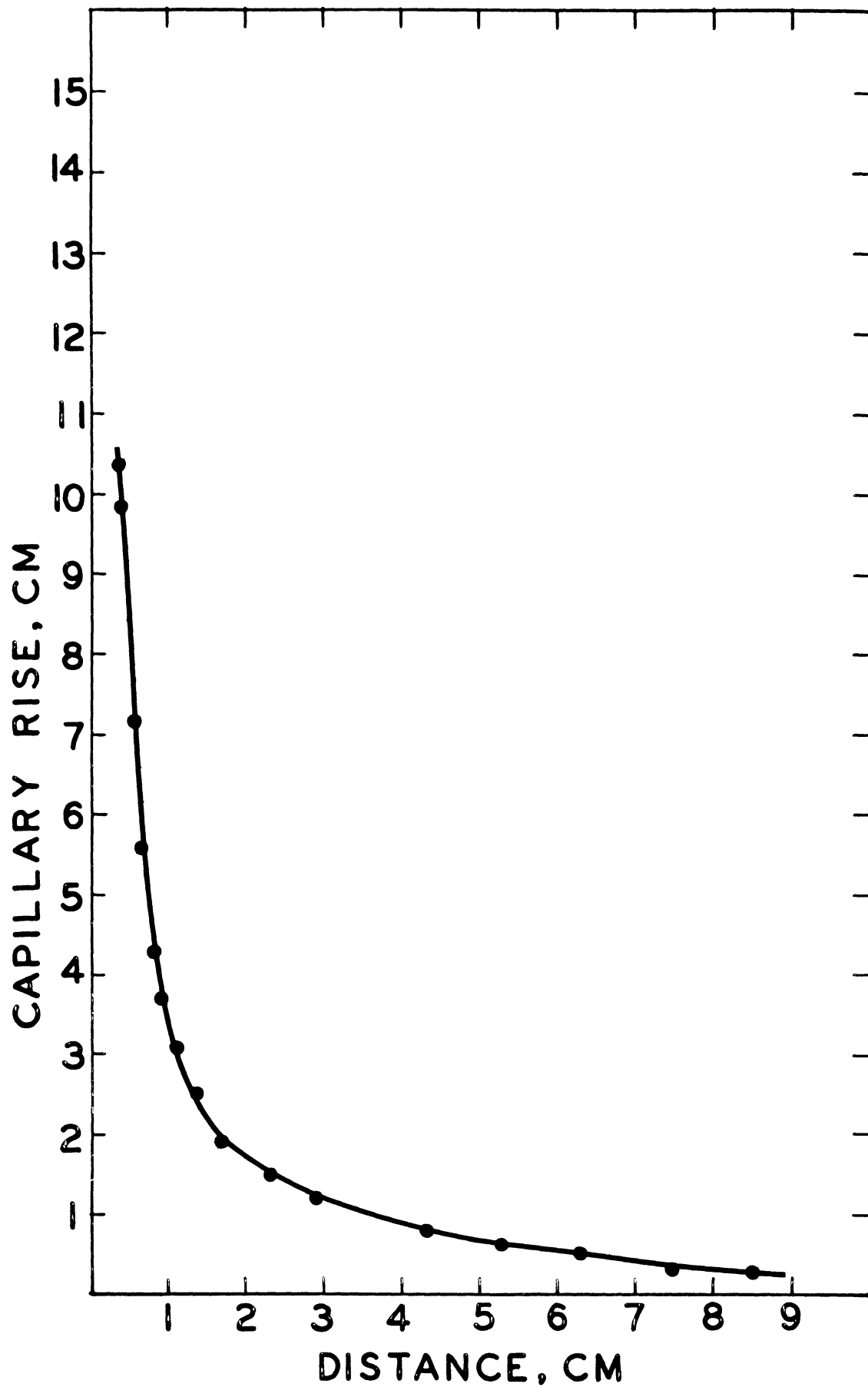


Figure 28. Capillary Rise Curve for Acrylic-Iodobenzene-Glass.  
 $\phi = 38'$ .  $\bar{x}h = 3.32$  sq. cm.



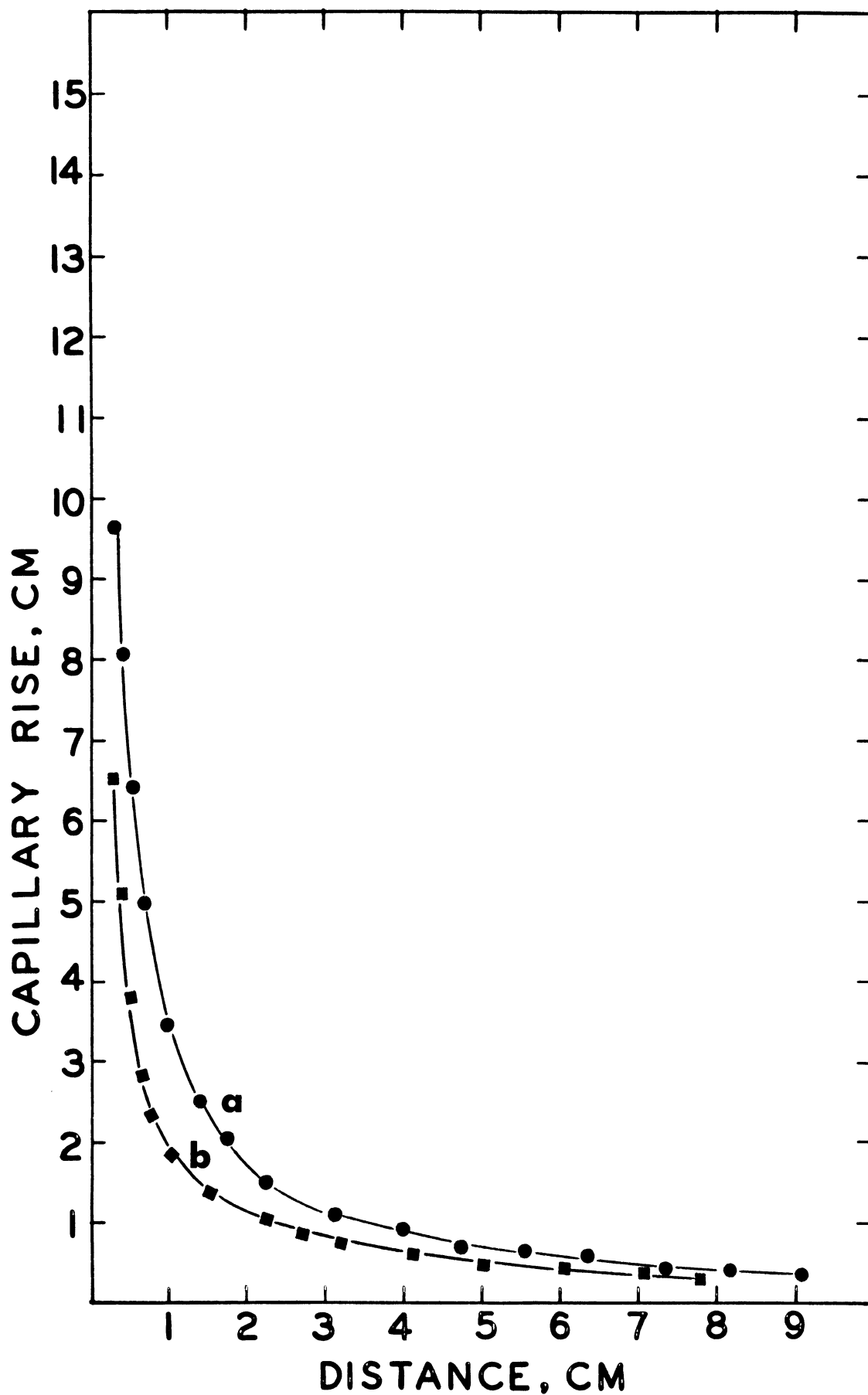


Figure 29. Capillary Rise Curves for: (a) Glass-Iodobenzene-Glass,  $\bar{x}h = 3.37$  sq. cm.; (b) Teflon-Iodobenzene-Glass,  $\bar{x}h = 2.19$  sq. cm.  $\theta = 38'$ .

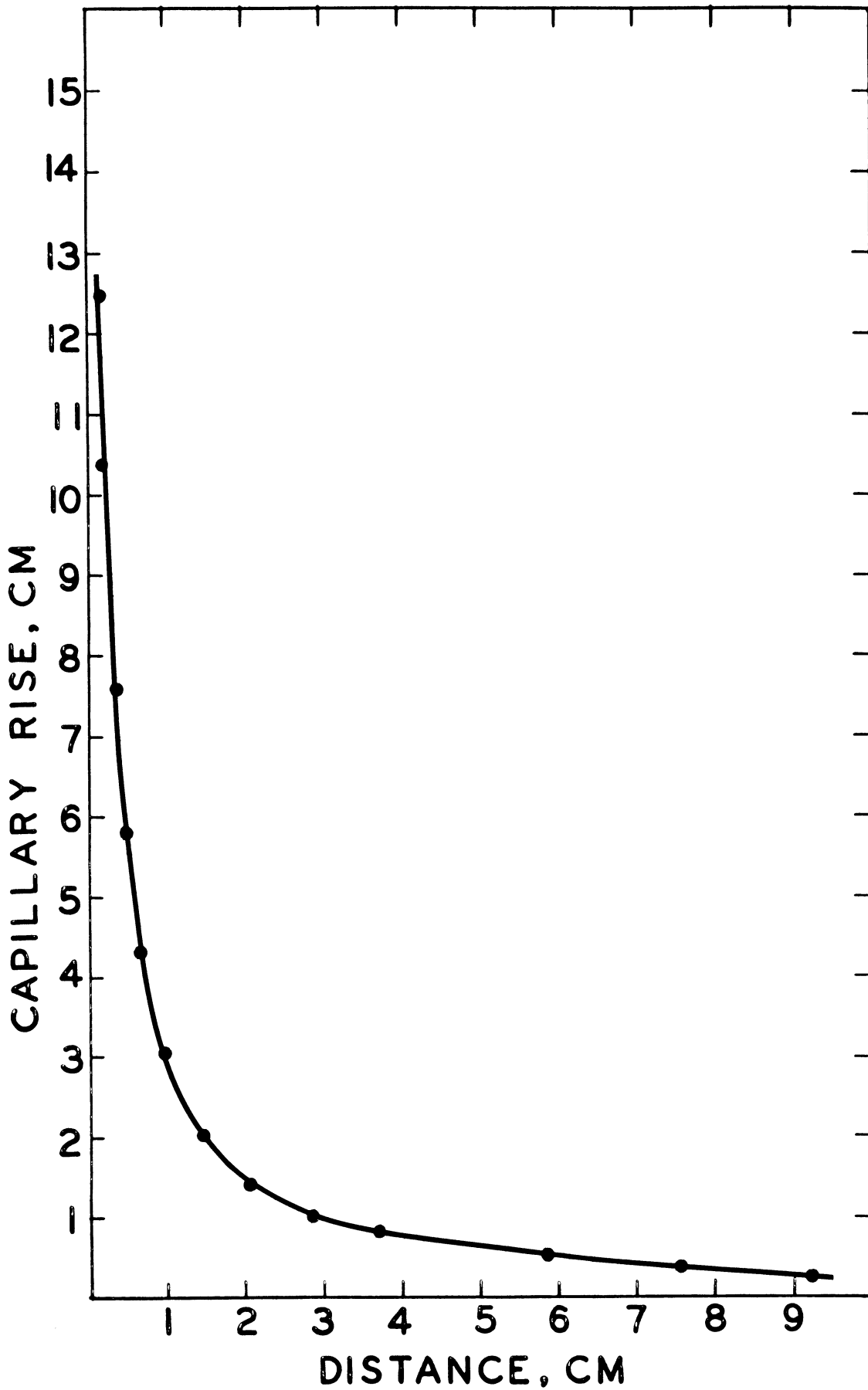


Figure 30. Capillary Rise Curve for Acrylic-Iodobenzene-Glass.  
 $\phi = 38'$ .  $\bar{x}h = 2.95$ .

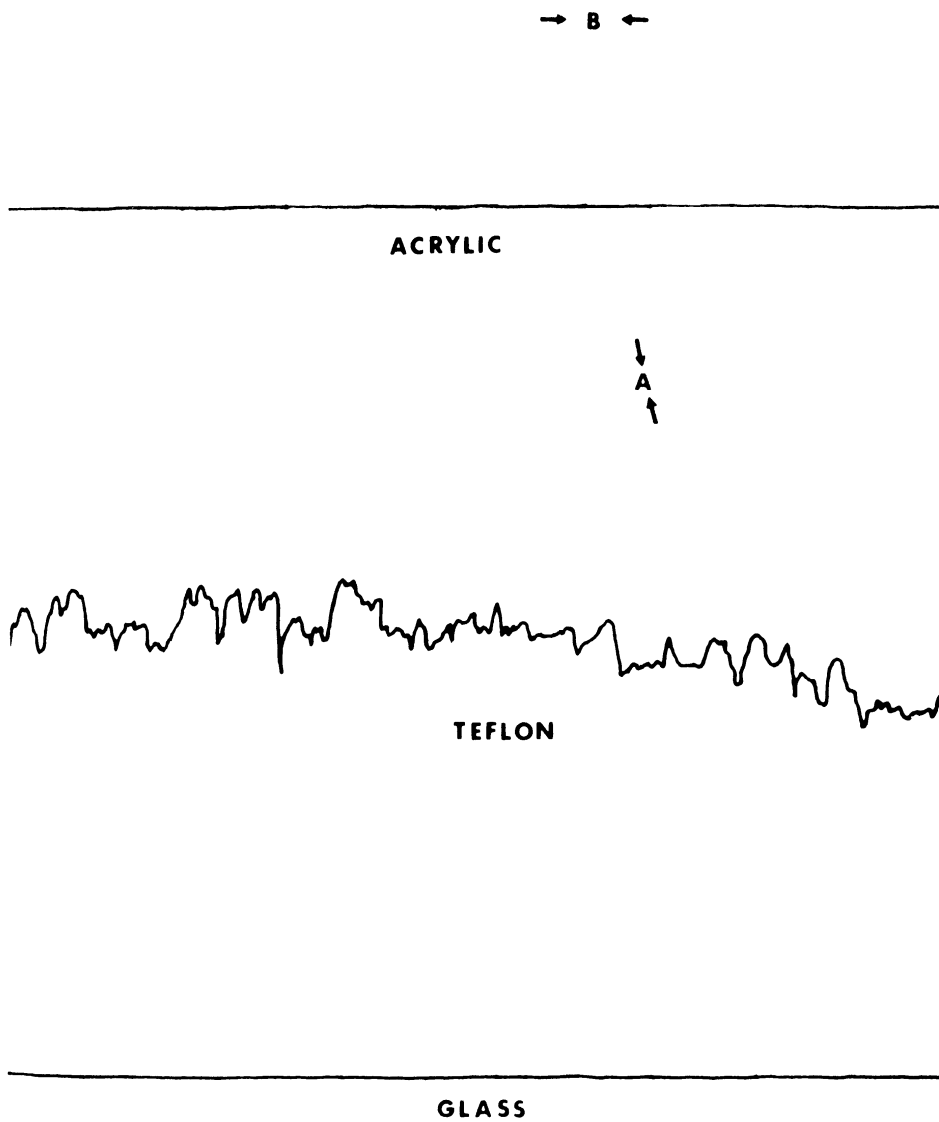


Figure 31. Surface Profiles Obtained From Surface Analyzer.  
A = 0.000125"; B = 0.010".

## VI. EVALUATION OF THE MODEL

In order to evaluate the newly derived mathematical model for liquid penetration between dissimilar plates, it is necessary to estimate its predictive ability. This may be done by substituting the values of the contact angles and surface tensions into the prime equation and solving for  $xh$ , the constant of the hyperbolic curve described by the meniscus of the liquid, then,

$$xh = \frac{\gamma_{LV} (\cos\theta_1 + \cos\theta_2)}{2 d \tan \phi/2 g} . \quad (26)$$

The advancing contact angle values for the three liquids on acrylic, glass, Teflon and silicone treated glass along with the determined surface tensions and known densities (0.79, 1.82, and 1.00 grams per cubic centimeter for ethanol, iodobenzene and water) were substituted in Equation 26. Following this procedure, the  $xh$  values shown in Table 6 were calculated. These values were plotted against those obtained by experiment in Figure 32.

### A. Regression Analysis

The first step in testing for the degree of association between the predicted and experimentally determined values, was to calculate the equation of the regression line that best fit the data points. Using the least squares method, the regression line for the observed values of  $(xh)_o$  on the predicted values,  $(xh)_p$  was found to be:

$$(xh)_o = 0.91 (xh)_p + 0.30 . \quad (28)$$

TABLE 6

PREDICTED AND OBSERVED  $x_h$  VALUES, sq. cm.

	Water			Iodobenzene			Ethanol			
	Glass	Teflon	Acrylic	Glass	Teflon	Acrylic	Glass	Teflon	Acrylic	
GLASS	13.60*	4.20*	8.25*	6.84*	3.88*	2.92*	3.94*	5.26*	4.73*	7.45*
	13.20+	3.32+	8.09+	6.93+	3.37+	2.20+	2.95+	5.45+	4.40+	7.55+
	12.63+			6.35+						10.60*
ACRYLIC	7.01*	-0.70*	3.47*	4.04*	3.94*	2.92*	3.88*	5.26*	4.73*	5.26*
	7.34+	0.0+	3.44+	3.81+	3.32+	2.82+	3.32+	5.05+	4.18+	4.08+
										9.36+

\* Predicted values.

+ Mean observed values.

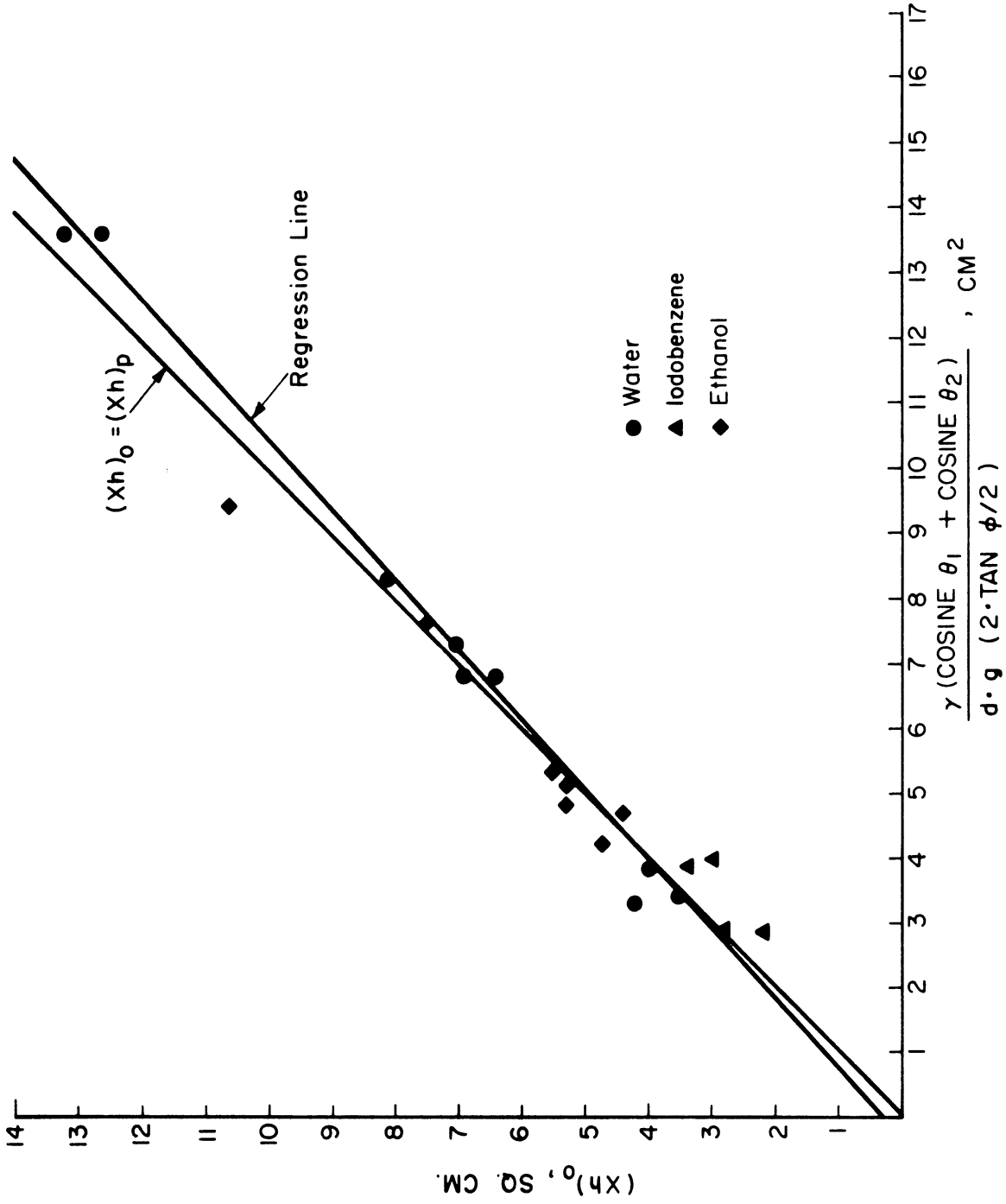


Figure 32. Regression of Observed  $\bar{x}_h$  Values on Calculated  $\bar{x}_h$  Values.

This line is drawn through the data in Figure 32 along with the line

$$(xh)_o = (xh)_p . \quad (29)$$

The slope of the regression line, 0.91, is close to unity indicating the values  $(xh)_o$  and  $(xh)_p$  are close to being in a 1:1 correspondance. In order to test the significance of this slope, a Student's  $t$  test was used. At  $t$  value of 30 was obtained with 21 degrees of freedom. This exceeded the critical  $t$  value at the 0.01 level of significance. The conclusion may be drawn, therefore, that the slope is significantly different from zero,

#### B. Correlation Coefficient

The absolute magnitude of a slope may be tested for significance, but there is no way to decide from the value of the slope alone whether a correlation is strong or weak. The strength of the correlation may be defined as the fraction of the total variance that is due to regression. An analysis of variance was used to obtain  $r$ , the correlation coefficient. The results of this analysis of variance when applied to the regression data of Figure 32 is summarized in Table 7. The value of  $r^2$  was obtained by dividing the regression variance component by the total variance, then

$$r^2 = \frac{339}{345} = 0.98 . \quad (30)$$

This statistical parameter indicates that 98 per cent of the variation in the regression data is due to a relationship between  $(xh)_o$  and  $(xh)_p$ . Although  $r^2$  gives the strength of the correlation directly in terms of a ratio of two variance components, it is nevertheless customary to

TABLE 7  
ANALYSIS OF VARIANCE FOR REGRESSION

Source of Variance	Sums of Squares	Degrees of Freedom	Mean Squares	F
Regression	339	1	339	970
Residual	6	21	0.35	
Total	345	22		



use the square root,  $r$  (known as the correlation coefficient) instead. The value of  $r$  may vary from zero (no correlation) to +1 (perfect positive correlation). In the present case,  $r$  was found to be 0.99. This corresponds to an  $F$  value of 970 which was highly significant at the 0.001 level.

Therefore, the predicted values obtained with Equation (26) correlated highly and significantly with the observed values in almost a 1:1 ratio. In summary, the model appears to be satisfactory.

The error, or unexplained variance may be due to errors in measurement of the parameter values or in the determination of the capillary rise. The greatest variation from the predicted values are found with systems containing Teflon. The most likely cause for this greater variation is the surface unevenness of the Teflon plates. As shown in Figure 31, the roughness and waviness are greater for this material than for acrylic or glass. Such surface unevenness introduces errors in the estimated angle between the plates. Another possible source of error is in the simplifying assumption that the weight of the meniscus above the lowest portion was insignificant. This assumption is also made in the derivation of the Young-Laplace equation. It is justified as long as the distance between the plates is small. This distance is usually taken to be approximately 1 millimeter. Since the spaces between the plates were less than 1 millimeter, this assumption is justified.

However, the aim of the experimental design employed was to gain an accurate estimate of the error variance rather than to concentrate on minimizing its magnitude. And, as the analysis of variance results indicated, the effect was significantly greater than the error variance.

## VII. DISCUSSION AND APPLICATION OF RESULTS

### A. General Discussion of Proposed Equation

The proposed Equation (21) shows to what degree a liquid will penetrate between two solids, at equilibrium. This equation casts light on the relation between the wetting of two materials and capillary pressure. By deriving the equation on the basis of the free energy change occurring at the solid-liquid interface, a knowledge of the radius of curvature of the liquid-gas interface is not necessary. This model teaches that the free energy change accompanying wetting is the driving force for capillary penetration. An examination of a few specific systems will illustrate this. Consider what occurs when water is allowed to penetrate between two glass plates. Using Equation (17) the following is found:

$$(F_{SV} - F_{SL}) + (F_{SV} - F_{SL}) = \Delta F^S = \gamma_{LV} (\cos\theta_1 + \cos\theta_2) \quad (31)$$

or

$$\Delta F^S = -136 \text{ ergs/cm.}^2 \quad (32)$$

This driving force produces the rise curve shown in curve "a" of Figure 10.

Now substitute a silicone coated glass plate ( $\theta_2 = 91^\circ$ ) for a glass plate, and the free energy change per unit area becomes,

$$\Delta F^S = -68.9 \text{ ergs/cm.}^2 \quad (33)$$

The result of this substitution is a smaller free energy change and a reduced capillary rise as shown in curve "b" of Figure 10. Next, a

plate of Teflon was paired with a glass plate, and here

$$\Delta F^S = -44.3 \text{ ergs/cm.}^2 \quad . \quad (34)$$

The capillary rise curve obtained is curve "c" in Figure 10. Plotting  $\Delta F^S$  against the  $(xh)$  values obtained with water and various combinations of plates in Figure 33, the relationship between  $\Delta F^S$  and capillary rise is illustrated.

Iodobenzene and ethanol produced less marked effects than water. Curve "a" in Figure 29 is the capillary rise curve obtained with the system glass-iodobenzene-glass. Upon substituting a Teflon plate for one of the glass plates, capillary rise curve "b" was obtained. Compared with the water systems, there was a less marked decrease in rise. This is due to the lower contact angle between iodobenzene and Teflon. Figure 34 is a pictorial representation of the relation between capillary rise, gap distance and the contact angles for water between two plates.

#### B. Leakage of Wax Fillings

Current theory holds that unless a material adheres to tooth tissue, leakage of mouth fluids will occur. The autoradiographic techniques described previously<sup>(18,19,20,21,22)</sup> have been the chief tools for testing for this adhesion. This approach has inherent pitfalls. First of all, capillary penetration depends for its driving force on the free energy decrease produced by wetting. If  $\Delta F^S$  is positive, penetration will not be spontaneous. If as shown in the experiment with wax fillings presented previously in this paper, the cavity wall is coated with wax and a wax filling is placed, penetration was prevented. However, the absence of penetration could only be demonstrated if the floor of the cavity was sealed as in treatment 3. This indicates

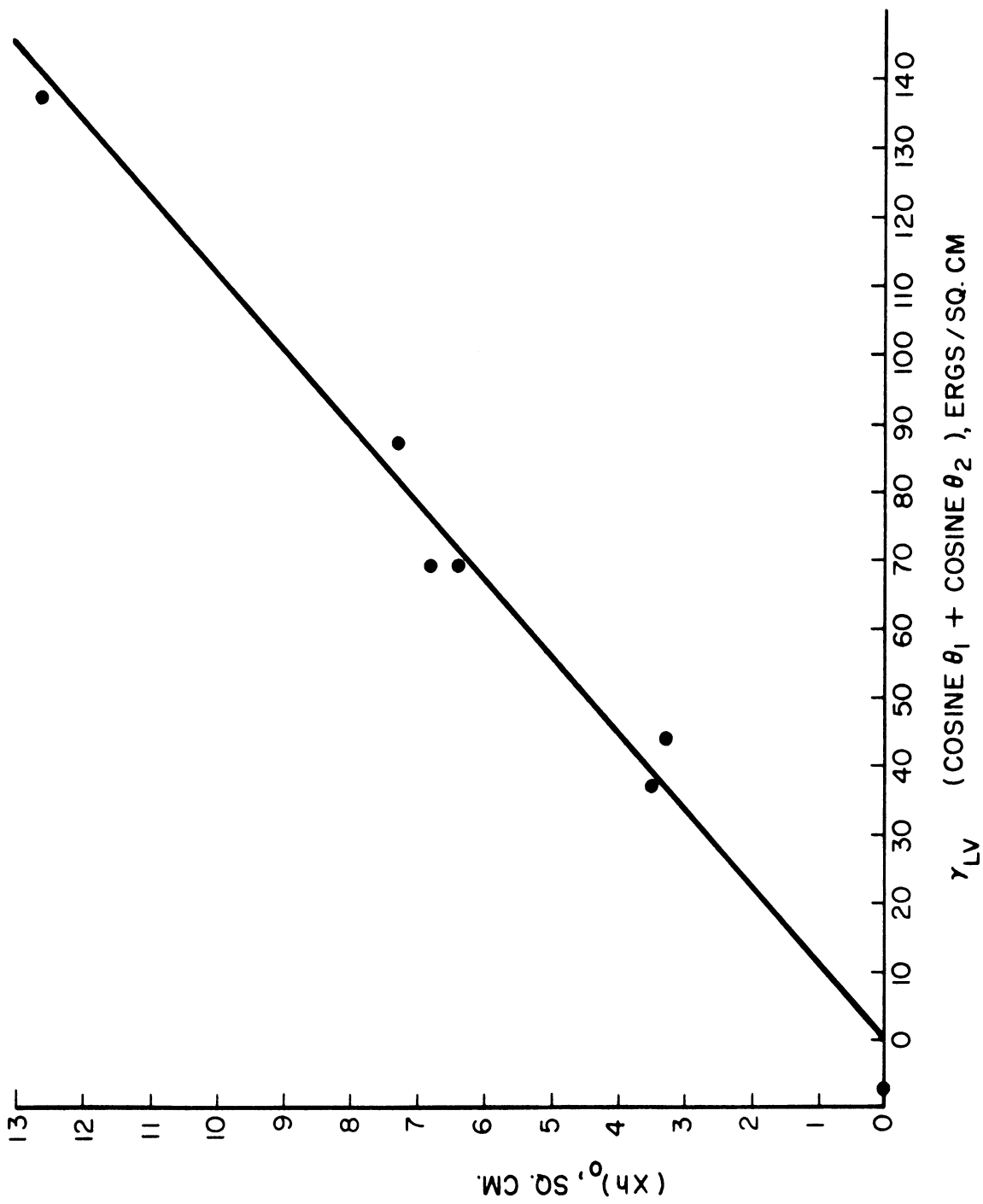


Figure 33. Observed  $\bar{x}h$  Values Versus Interface Free Energy Change Per Unit Area for Water.

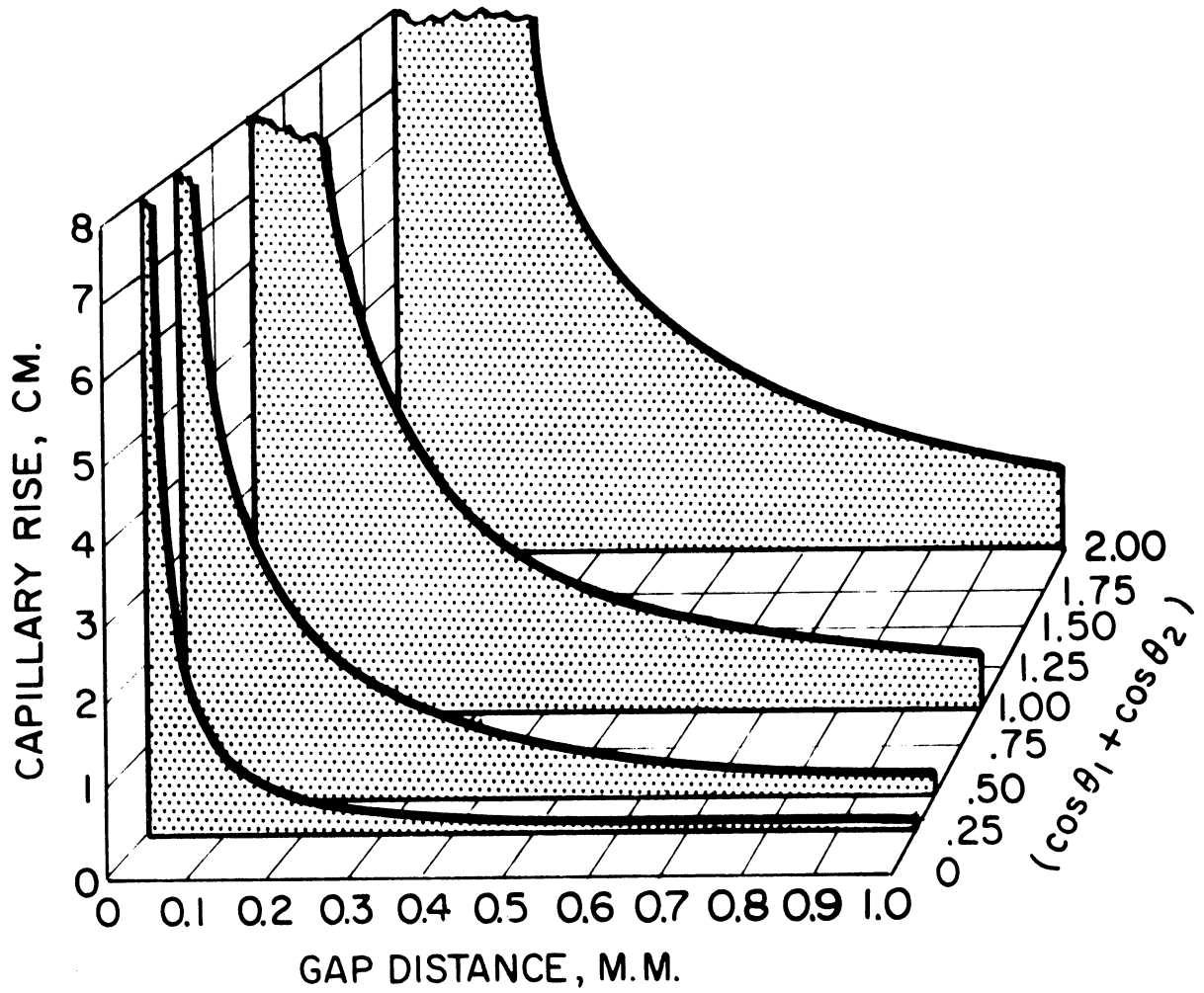


Figure 34. Capillary Rise Curves for Water Between Two Plates for Different  $(\cos \theta_1 + \cos \theta_2)$  Values.

that penetration by the isotope solution occurs by routes other than around the fillings. One probable route is through the root canal and auxillary root canals. It is exceedingly difficult to close off these paths of penetration. Another path is through the cementum or along the enamel-cementum junction. Also penetration through cracks in the enamel produced during the cavity preparation are likely channels for penetration. Filling these cracks with wax will not prevent penetration as indicated in the results of treatment 1. As a consequence of the many possible sources for penetration of isotope, experiments without controls are suspect.

C. Leakage Around Dental Materials

Considering the free energy change per unit area accompanying the penetration of water between dentin and various materials is instructive. Uy and Chang<sup>(36)</sup> have reported values for the contact angle of water on human dentin. Their results ranged from values of 13 degrees to 80 degrees. If for heuristic purposes, the contact angle of water on dentin is taken as 50 degrees, values of

$$\gamma_{LV} (\cos\theta_1 + \cos\theta_2) \quad (35)$$

may be calculated using 71 ergs/cm<sup>2</sup> as the surface energy of water and the contact angle values in Table 2. The results are listed in Table 8. These data indicate the relative free energy driving force for the capillary penetration of water between the material listed and dentin with a contact angle of 50°. The relatively low value, found for amalgam is most likely due to the presence of low energy surface reaction products.

TABLE 8

VALUES OF  $\Delta F^S$  FOR THE PENETRATION OF  
WATER BETWEEN DENTIN ( $\theta = 50^\circ$ ) AND  
VARIOUS MATERIALS

Material	$\Delta F^S = \gamma_{LV} (\cos\theta_1 + \cos\theta_2)$ ergs/cm <sup>2</sup> .
Filling Porcelain	-116
Bonfil	-103
Addent	-90
Acrylic Resin	-65
True Dentalloy	-61
Teflon	-20

Of course, the situation in vivo will involve saliva rather than water. These calculations, therefore, merely illustrate the approach that may be used in considering this problem.

These data indicate that treatment of dentin to render its surface hydrophobic is necessary to prevent penetration even when Teflon is used as the second material. Also, since the crevices formed around dental fillings are usually microscopic in dimensions, kinetic factors take on importance. Further work in this area is needed. Also, more fundamental information on the behavior of dentinal fluids under restorations is needed.

#### D. Denture Retention

The equation relating the force necessary to separate two plates separated by a film of liquid has been given as

$$f = \frac{2 \gamma_{LV} \cos\theta A}{bg} = \Delta P A \quad (14)$$

If dissimilar materials are involved, the equation becomes

$$f = \frac{\gamma_{LV} (\cos\theta_1 + \cos\theta_2) A}{bg} \quad (36)$$

Therefore, the maximum retention will be obtained when both contact angles are zero for a given liquid. In the present case, materials that are readily wetted by saliva will produce the highest values of capillary retention.



### VIII. SUMMARY

- (1) A mathematical model for the capillary penetration of liquids between plates of dissimilar materials was derived from free energy consideration. The proposed equation is:

$$h = \frac{\gamma_{LV} (\cos\theta_1 + \cos\theta_2)}{b d g} . \quad (21)$$

- (2) The above equation was modified to deal with the capillary penetration between dissimilar plates that are at an angle  $\phi$  with each other:

$$xh = \frac{\gamma_{LV} (\cos\theta_1 + \cos\theta_2)}{2 d g \tan \phi/2} , \quad (26)$$

where  $x$  represents the horizontal distance from the vertex of the two plates.

- (3) Advancing and receding contact angles for water, iodobenzene and ethanol on glass, silicone, acrylic, resin, and poly-(tetrafluoroethylene) were determined by the tilting plate method. The results for advancing contact angles agreed with published values, when available.
- (4) Surface tensions of water, iodobenzene, and ethanol were determined by the ring method. The observed values agreed with published results.
- (5) The observed surface tension and contact angle values were substituted in Equation (26) and predicted ( $xh$ ) values were calculated.
- (6) The capillary rise between two plates at a small angle to each other was measured at several distance from the vertex. A factorial

design was used in which permutations of plate materials and liquids were tested. A coordinate cathetometer was used to measure the rise.

- (7) In order to evaluate the proposed equation, the agreement between the predicted and average  $(xh)$  values was tested by means of regression and correlation analysis. These statistical tests indicate a highly significant correlation between the predicted and observed  $(xh)$  values. These results were presented as evidence that the proposed equation was a satisfactory one for the systems tested.
- (8) The proposed Equations (21) and (26) were tested by dimensional analysis and found to be homogeneous and complete equations.
- (9) The contact angles of water on a variety of dental materials was determined using the tilting plate method. Of the dental materials tested, dental amalgam gave the highest contact angle values.
- (10) Experiments on the penetration of an aqueous solution containing  $^{14}\text{C}$  around wax fillings in extracted teeth were performed. Quantitative measurements of the relative amounts of penetration were assessed with a liquid scintillation spectrometer. Variance tests were used to draw conclusions from the data. The statistical evidence indicated that the interpretation of marginal penetration is more complex than had been previously assumed and that water penetration was prevented by coating the surface of the cavity with wax and using a wax filling.
- (11) The penetration of mouth fluids around dental restorations was discussed in terms of the proposed mathematical model. The free

energy changes per unit area accompanying capillary penetration of water between dentin and several dental materials were calculated for heuristic purposes.

- (12) An equation was proposed for the adhesion of dissimilar plates by a thin film of liquid. The force necessary to separate the plates of area  $A$  was found to be,

$$f = \frac{\gamma_{LV} (\cos\theta_1 + \cos\theta_2) A}{b g} . \quad (35)$$

- (13) Denture retention in the light of the above equation for adhesion was discussed briefly.

## REFERENCES

1. Van Valkenburg, J. W., Jr., Factors That Influence the Magnitude of the Contact Angle. Ann Arbor, University of Michigan, Chemistry, 1954, 109 p. (p. 1) typed thesis.
2. Davis, J. T., and Rideal, E. K., Interfacial Phenomena. 2nd ed., New York, Academic, 1963, 480 p., (p. 35).
3. Kawaski, K., "Study of Wettability of Polymers by Sliding of Water Drops." J. Coll. Sci., 15, 402-407, October, 1960.
4. Shepard, J. W., "The Effect of Surface Roughness on Apparent Contact Angles and on Contact Angle Hysteresis." Ann Arbor, University of Michigan, Chemistry, 1952. 133 p. (p. 20).
5. Van Valkenburg, Op. Cit., p. 6.
6. Davis and Rideal, Op. Cit., p. 38.
7. Macdougall, G., and Ockrent, C., "Surface Energy Relations in Liquid Solid Systems." Proc. Roy., 180A, 151-73, 1941.
8. Moore, W. J., Physical Chemistry., Englewood Cliffs, Prentice-Hall, 1963, 844 p. (p. 730).
9. Adamson, A. W., Physical Chemistry of Surfaces., New York, Wiley, 1960, 629 p (p. 4-6).
10. Adamson, Op. Cit., p. 13.
11. Adamson, Op. Cit., p. 14-16.
12. Conant, J. B., Science and Common Sense., New Haven, Yale, 1951, 344 p. (p. 86).
13. Ditton, Humphrey, The New Law of Fluids., London, Ward, 1729.
14. Grunmach, Leo, "Uber einen neuen Plattenapparat zur Bestimmung von Kapillaritätskonstanten nach der Steighohenmethode." Physik. Zeit., XI: 980-989, 1910.
15. Owen, E. A., and Durfton, A. F., "The Application of Radiography to the Study of Capillarity." Proc. Phys. Soc., (London) 38: 204-206, 1925-26.
16. Bakker, G., Kapillarchemie, p. 71-83 (In Handbuch der Physik. VI, Leipzig, Wien-Harmsschen, 1928).

17. Wolf, K. L., Physik und Chemie der Grenzflächen., Berlin, Springer, 1957.
18. Phillips, R. W., Gilmore, H. W., Swartz, M. L., and Schenker, S. I., "Adaption of Restorations In Vivo as Assessed by  $^{45}\text{Ca}$ ." Am. Dent. A. J., 62, 9-20, Jan. 1961.
19. Lyell, J., Barber, D. B., and Massler, Maury, "Effect of Saliva and Sulfide Solution on the Marginal Seal of Amalgam Restorations." J. Dent. Res., 43:375-379, 1964.
20. Going, R. E., Massler, Maury, "Influence of Cavity Liners Under Amalgam Restorations on Penetration by Radioactive Isotopes." J. Prosth. Dent., 11, 298-312, 1961.
21. Cantwell, J. C., Cantwell, K. R., "Study of Marginal Seal of Dental Restorations using  $^{14}\text{C}$  Labeled Fructose." J. Dent. Res., 38, 755, 1959.
22. Going, R. E., and Massler, Maury, and Dute, H. L., "Marginal Penetration by Different Radioactive Isotopes." J. Dent. Res., 39, 273-284, 1960.
23. Fiasconaro, J. E., and Sherman, H., "Sealing Properties of Acrylics." N.Y.S. Dent. J., 18, 198, 1952.
24. Pinto, J. and Bunocore, M. G., "Effect of Base and Cavity Liners on Marginal Leakage of Filling Materials." N.Y.S. Dent. J., 28, 199-208, 1963.
25. Nelsen, R. J., Wolcott, R. B., and Paffenbarger, G. C., "Fluid Exchange at the Margins of Dental Restorations." Am. Dent. A. J., 44, 288-298, 1952.
26. Harrison, L. M., Bacterial Penetration of Varnish-Lined Amalgam Restorations., Ann Arbor, University of Michigan, School of Dentistry, thesis, 51 p., 1964.
27. Mortensen, D. W., Boucher, N. E., and Ryge, Gunnar., Method of Testing for Marginal Leakage of Dental Restorations with Bacteria., I.A.D.R. Gen. Meeting, 1963, abstracts, p. 34.
28. Ostlung, S. G., "Some Physical Principals in the Retention of Dentures." Northwestern Univ. Bull., 49, 11-19, 1948.
29. Craig, R. G., Berry, G. C. and Peyton, F. A., "Physical Factors Related to Denture Retention." J. Pros. Dent., 64, 541-543, 1960.
30. O'Brien, W. J., and Ryge, Gunnar, "Wettability of Poly-(Methylmethacrylate) Treated with Silicon Tetrachloride." J. Prosth. Dent., 15, 304-308, March, 1965.

31. Roydhouse, R. H., "The Retention of Dentures," Am. Dent. A. J., 59, 159-163, 1960.
32. Perry, J. H., ed. Chemical Engineers' Handbook., 3rd. ed., New York, McGraw-Hill, 1950, 1429p. (p. 93-97).
33. Fisher, R. A., Statistical Methods for Research Workers., London, Oliver and Boyd, 10th ed., 1946.
34. Hodgeman, C. D., editor, Handbook of Chemistry and Physics, ed. 44, Cleveland, Chemical Rubber Pub., p. 2233, 1962.
35. Steel, R. G., and Torrie, J. H., Principles and Procedures of Statistics., New York, McGraw-Hill, 1960, 481 p. (p. 107).
36. Uy, K. C., and Chang, R., An Approach to the Study of the Mechanism of Adhesion to Teeth. p. 103-128. (In Adhesive restorative dental materials - II. Bethesda, National Institute of Dental Research. 1965., 293 p.)